A 20-Year Climatology of Nocturnal Convection Initiation over the Central and Southern Great Plains during the Warm Season

DYLAN W. REIF AND HOWARD B. BLUESTEIN

School of Meteorology, University of Oklahoma, Norman, Oklahoma

(Manuscript received 31 August 2016, in final form 20 January 2017)

ABSTRACT

A nocturnal maximum in rainfall and thunderstorm activity over the central Great Plains has been widely documented, but the mechanisms for the development of thunderstorms over that region at night are still not well understood. Elevated convection above a surface frontal boundary is one explanation, but this study shows that many thunderstorms form at night without the presence of an elevated frontal inversion or nearby surface boundary.

This study documents convection initiation (CI) events at night over the central Great Plains from 1996 to 2015 during the months of April–July. Storm characteristics such as storm type, linear system orientation, initiation time and location, and others were documented. Once all of the cases were documented, surface data were examined to locate any nearby surface boundaries. The event's initiation location relative to these boundaries (if a boundary existed) was documented. Two main initiation locations relative to a surface boundary were identified: on a surface boundary and on the cold side of a surface boundary; CI events also occur without any nearby surface boundary. There are many differences among the different nocturnal CI modes. For example, there appear to be two main peaks of initiation time at night: one early at night and one later at night. The later peak is likely due to the events that form without a nearby surface boundary. Finally, a case study of three nocturnal CI events that occurred during the Plains Elevated Convection At Night (PECAN) field project when there was no nearby surface boundary is discussed.

1. Introduction

Precipitation is most frequent at night over the central Great Plains during the warm season (Kincer 1916; Wallace 1975; Easterling and Robinson 1985; Riley et al. 1987; Carbone et al. 2002; Carbone and Tuttle 2008). Much of the precipitation has been attributed to mesoscale convective systems (MCSs; Fritsch et al. 1986).[1] Carbone and Tuttle (2008) showed that the average precipitation frequency during June, July, and August between 1996 and 2007 was highest over the lee of the Rockies during the late afternoon, was highest over the central Great Plains just after midnight, and that the longitudinal area between 102° and 90°W had the highest frequency of nocturnal convection. The most common time of precipitation has been shown to range from 0500 to 0800 UTC (0000–0300 LST) in the central Great Plains region during the warm season (Wallace 1975; Easterling and Robinson 1985; Riley et al. 1987; Fabry 2012). However, this time represents *both* preexisting systems that move through the region and convection that is initiated in the region.

Over the Great Plains, MCSs have a large nocturnal component (Maddox 1980), and tend to occur in regions of strong low-level warm advection (Maddox 1983) These systems account for between 30% and 70% of warm-season precipitation (Fritsch et al. 1986). Maddox et al. (1979) described a type of flooding event in which warm, moist air flows over an east–west-oriented quasi-stationary front and is often downstream from a low-level jet (LLJ) maximum and in a later study (Maddox 1983) showed that the LLJ is a common precursor to MCS development.

Elevated convection, which is defined as convection whose source of lift is not rooted in the boundary layer, is common at night during the warm season (Colman 1990a,b).

[1] Their study considered MCSs to be a subset of the larger mesoscale convective complex (MCC), but the current understanding considers MCCs to be a subset of MCSs [see Markowski and Richardson (2010) their Fig. 9.4].

Corresponding author e-mail: Dylan W. Reif, dylanreif@ou.edu

DOI: 10.1175/MWR-D-16-0340.1

In his 5-yr study, the peak occurrence of elevated convection was in eastern Kansas and the majority of cases occurred 1°–2° latitude (approximately 100–200 km) north of a quasi-stationary front. During the International H_2O Project (IHOP_2002; Weckwerth et al. 2004), approximately 80% of all nocturnal convection initiation (CI) events were elevated (Wilson and Roberts 2006). They suggested that a zone of elevated convergence combined with areas of midlevel instability provided conditions for elevated convection to form with no nearby surface boundary.

Even though elevated convective systems typically occur above a nocturnal stable layer, they still produce severe weather, including tornadoes and severe-wind events. Grant (1995), who first studied the relationship between elevated convection and severe weather, showed that the majority of severe-storm reports were associated with hail, but he examined only 11 severe cases over a 3-yr period. Horgan et al. (2007) expanded Grant's study by formulating a 5-yr climatology of elevated convection that produced severe weather. As in Grant's study, they showed that the majority of severe-storm reports were from hail and they also showed that only one-third of the severe reports were from high wind. They hypothesized that the relative lack of severe-wind events is associated with a near-surface stable layer, which limits the potential for high winds aloft to penetrate to the surface. In their study, the severe events had a peak occurrence in May and a secondary peak in September. While the majority of the events occurred in the late afternoon, many events occurred during the night.

Nocturnal CI and elevated CI are still major forecasting problems (Davis et al. 2003; Trier et al. 2006; Surcel et al. 2010). One reason is that mesoscale features such as outflow boundaries and horizontal convective rolls (HCRs) are poorly sampled and are poorly resolved in many operational models (Trier et al. 2014). Another complication is that the processes that lead to CI during the day are not as effective at generating convection at night. Features such as the LLJ and gravity waves (including atmospheric bores) are more important in generating nocturnal convection (Marsham et al. 2011). Many models focus on processes important to surface-based convection and are not as effective at correctly capturing nocturnal convection (Anderson et al. 2002).

The nocturnal LLJ (Blackadar 1957; Wexler 1961; Holton 1967; Bonner 1968) has been shown to influence CI. In a case study of the 3–4 June 1985 MCS over southern Kansas and northern Oklahoma it was shown that the LLJ transported warm, moist air over a quasi-stationary front, destabilizing the environment (Trier and Parsons 1993). More recently, Tuttle and Davis (2006) showed that nocturnal CI is confined to a narrow longitude area between 100° and 95°W, a common location for the LLJ. As the strength of the LLJ increased, the rainfall increased and more systems formed in the region than moved into the region.

This study is the first long-term climatology of nocturnal CI over the central and southern Great Plains during the warm season. Limiting the spatial area and time frame to the most affected area allows for a more detailed climatology representative of a specific region. Furthermore, this study focuses only on storm characteristics at *initiation*. How these characteristics change throughout each storm's life cycle was not documented. The objectives of this paper are 1) to formulate a 20-yr (1996–2015) climatology of nocturnal CI over the central and southern Great Plains during the warm season, 2) to identify different modes of nocturnal CI, and 3) to identify different environmental characteristics among the modes. The methods are described in section 2, the climatology is presented in section 3, a brief discussion is presented in section 4, a case study is presented in section 5, and conclusions of this study and an introduction to the next paper in a two-part series are presented in section 6.

2. Methods

CI events, classified as precipitating convective storms that have a maximum radar reflectivity factor of at least 40 dBZ, were documented over the central and southern Great Plains region (Fig. 1) during the night. The Rossby radius of deformation (NH/f), where N is the Brunt–Väisälä frequency, H is a characteristic depth, and f is the Coriolis parameter, is approximately 100 km, assuming that the scale height is the characteristic depth of ~10 km (H) and that there is a near-surface stable layer characterized by an increase in potential temperature with height of 10 K $(300\ \text{m})^{-1}$. If air flows at 15 m s^{-1}, then it takes just over 2.5 h to travel 100 km. The Rossby radius of deformation is used to identify objectively what may be considered "pristine" convection (convection that is not influenced by other neighboring convective storms). For this study, CI events that occurred within 100 km and within 3 h of the main event are counted as the same event.

Night is defined as the time between just after local sunset to just before local sunrise. Unlike many previous studies, this is not two set times (i.e., 0000 and 1200 UTC). It depends on the day of the year and the location, allowing for a more fluid and accurate classification of

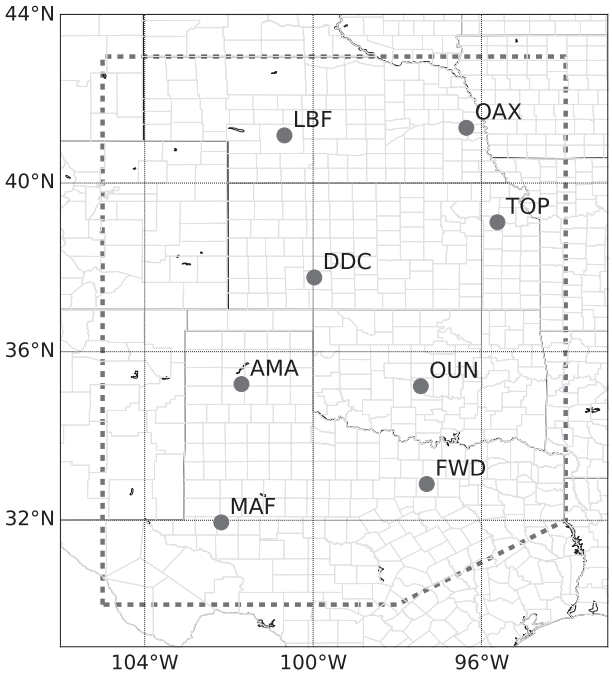

FIG. 1. The area of concern (outlined in the dashed gray box). The locations of NWS sounding stations used are denoted by the gray dots.

nocturnal CI events. The spatial extent of the domain was chosen because that area has been shown to have more cases of nocturnal convection than the surrounding areas and is altered near the Texas–Gulf Coast to remove the effects of sea/land breezes. The warm season, defined here as April–July, was chosen because much of the nocturnal convection over the Great Plains occurs during that time period (Wallace 1975, Fritsch et al. 1986).

To identify the CI events,[2] radar composite data were examined from the UCAR MMM radar composite archive (available online at http://www2.mmm.ucar.edu/imagearchive/). The radar data are available in 30-min intervals for most days and only the central and southern Great Plains were considered. There are 118 510 images out of a possible 136 640, so the dataset is 86.7% complete. However, there are many days (including a nearly 6-month period between 1997 and 1999) when the data were available only in hour-long intervals, and days during which a few images are missing, but CI events can still be identified from those images. The dataset is then over 90% complete during the 20-yr period.

Surface data were examined using the Automated Surface Observing Station (ASOS) network and Oklahoma Mesonet (McPherson et al. 2007) data. Surface boundaries, including wind-shift lines, cold fronts, warm fronts, quasi-stationary fronts, outflow boundaries, drylines, and baroclinic zones [a temperature gradient of at least 10°C (100 km)$^{-1}$ with no wind shift] were identified and the CI location was marked relative to the surface boundary. If CI was on the cold side of a surface boundary, then the distance from the boundary was noted. If there was a surface boundary, but the CI occurred more than 700 km away, then that event was assumed to not be influenced by that surface boundary, since most vertical circulations about fronts and outflow boundaries are only on the order of several hundred kilometers or less (Bluestein 1993).

Three storm types were identified in this study: *areal*, *linear*, and *single cell*. These storm types were classified based on the type at initiation. For example, if a system began as a single cell and a few hours later grew upscale into an areal or linear system, it was classified as a single cell. The linear events are those for which the length of the radar echo is at least 5 times its width as in Bluestein and Jain (1985). The areal events are neither linear events nor single-cell events and include MCSs and mesoscale convective complexes (MCCs) (unless the MCS or MCC met the linear classification).

Severe events were classified using the previous National Weather Service (NWS) criteria.[3] On 5 January 2010, the NWS changed the severe-hail criterion to 1.00-in. diameter. However, since a hail diameter of 0.75 in. was the criterion for most of this study, that criterion was used for the entire climatology. Flooding events are also classified as severe events because they can have many negative impacts on life and property. In this study, the *number* of severe reports was not considered; only the *type* of severe report was in order to identify how often a severe event occurs with respect to all events. The severe reports had to occur at night during the storm's life cycle to be included in this study, but some cases had severe reports that occurred during the day as well.

Representative wind profiles were identified for over 90% of the events. To be classified as a representative wind profile, the sounding from which it came had to lie in the cold air for the events that

[2] It is important to note that the events documented in this study are not necessarily the same as the events documented in previous climatologies of elevated convection. Unlike other studies, this study focuses on a specific region of the United States during a specific time of the year and at night.

[3] These criteria were hail greater than 0.75 in. (1.9 cm) in diameter, wind speeds greater than or equal to 50 kt (25.7 m s^{-1}), and a tornado.

initiated on the cold side of a surface boundary and ahead of the boundary for the events that initiated on a surface boundary. The sounding also had to be within 3° latitude or longitude of the event (Horgan et al. 2007). To capture the nocturnal stable layer, many soundings were at 1200 UTC. If no representative wind profile could be identified at 0000 or 1200 UTC for the cases, then that case was not included in the representative wind profile analysis.

To classify the LLJ, the Bonner (1968) criteria were applied at the eight sounding stations shown in Fig. 1. Bonner (1968) used three criteria to classify the LLJ: a criterion-1 LLJ has a wind speed that equals or exceeds $12\,m\,s^{-1}$ and decreases by at least $6\,m\,s^{-1}$ at the next higher minimum or at 3 km, a criterion-2 LLJ has a wind speed that equals or exceeds $16\,m\,s^{-1}$ and decreases by at least $8\,m\,s^{-1}$ at the next higher minimum or at 3 km, and a criterion-3 LLJ has a wind speed that equals or exceeds $20\,m\,s^{-1}$ and decreases by at least $10\,m\,s^{-1}$ at the next higher minimum or at 3 km. There were many criterion-3 LLJs (the strongest LLJs in his study) in this study, so a fourth criterion was added to extend Bonner's criteria. A criterion-4 LLJ has winds that equal or exceed $24\,m\,s^{-1}$ and decrease by at least $12\,m\,s^{-1}$ at the next higher minimum or at the 3-km height, or whichever is lower. A final constraint was that the wind direction had to be approximately southerly (from 135° to 225°) at the level of peak wind intensity. The approximate center of the LLJ was placed at the station with the highest criteria LLJ. If two or more station reported the same criterion, then the approximate center was placed in the center of the stations.

3. Results

There were 930 pristine nocturnal CI events during the 20-yr period.[4] We define pristine CI as CI that is not influenced by other convection. The most common initiation time was 0500 UTC and the most common initiation month was July (Figs. 2a,b). Over half of all events were of the linear storm type, nearly 39% were of the areal storm type, and fewer than 10% were single cells (Fig. 2c). Three location-based CI modes account for over 80% of all CI events: at a surface boundary (AB CI mode) and on the cold side of a surface boundary (CS CI mode); CI also occurs with no nearby surface boundary (NB CI mode). Events in the CS CI mode [the Colman (1990a) definition of elevated convection] account for 35% of all events while the events in the AB CI mode and the events in the NB CI mode account for 23% and 24% of all events, respectively (Fig. 2d). The "other" mode includes events that initiate ahead of a moving boundary or on the warm side of a cold front or quasi-stationary front.

CI occurs primarily in the northern half of the domain, and the peak initiation location is in western Kansas and south-central Nebraska (Fig. 2e). There is a secondary peak initiation location in central Texas and southwestern Oklahoma. These events likely represent a different mode of CI from the events in Kansas and Nebraska and will be discussed later in this section. When the events initiate on the cold side of a surface boundary, the peak distance poleward of the boundary is between 100 and 200 km (Fig. 2f). This finding corresponds well with that of Colman (1990a).

Over one-third of all nocturnal CI events produce at least one severe-weather report (hail, wind, tornado, or flooding; not shown). Of the severe storms, hail is the dominant severe-weather type (accounting for over 30% of all events), wind and flood events are less common (accounting for 14% and 10% of all events, respectively), and tornadoes are rarely associated with nocturnal CI as there were only 11 tornado events (Fig. 2g). Hail events account for 84% of all severe events, wind events account for 38% of all severe events, tornado events account for 3% of all severe events, and flooding events account for 26% of all severe events (Fig. 10). These percentages correspond well with the past studies of severe, elevated convection even though the percentages represent events and not number of reports.

The LLJ is commonly associated with nocturnal CI events; over 70% of all events have an LLJ signature somewhere in the domain[5] (Fig. 2h). Just over 44% of CI events occur in environments with a weak (criterion 1 or 2) LLJ in the domain and 27.7% of events are initiated with a strong (criterion 3 or 4) LLJ in the domain. It is noteworthy that over 11% of the events are associated with a criterion-4 LLJ, justifying the need to extend the Bonner (1968) criteria.

In sections 3a–3h, the three storm-type modes (the areal storm-type mode, linear storm-type mode, single-cell storm-type mode) and the three location-based modes (the AB CI mode, CS CI mode, and NB CI mode) are discussed.

a. Initiation time

The peak initiation time for linear storm-type CI mode events, AB CI mode events, and CS CI mode

[4] For comparison, there were 497 events in the Colman (1990a) 4-yr climatology (some events had multiple reports) and 129 events in the Horgan et al. (2007) 5-yr climatology.

[5] Note that a criterion-0 LLJ represents no LLJ in the domain.

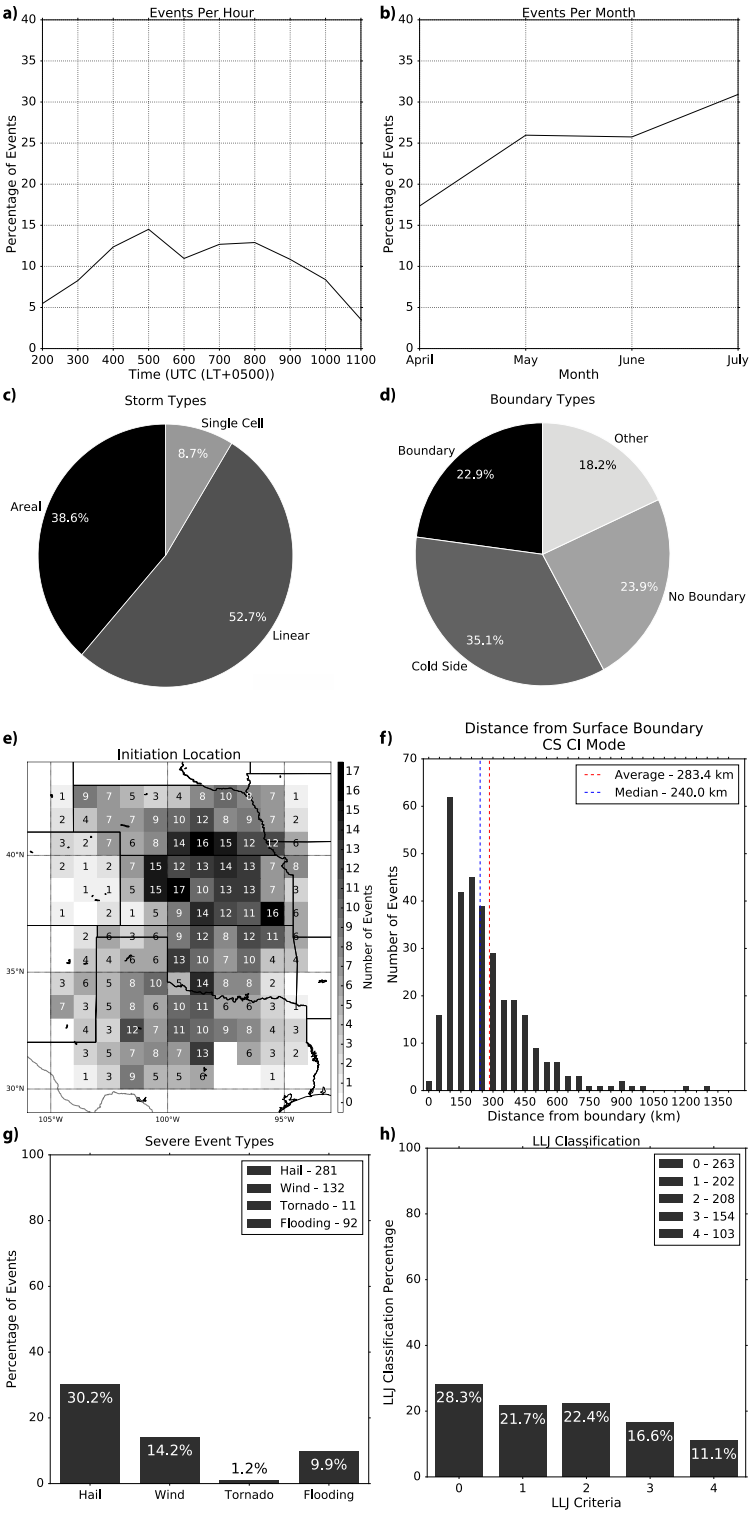

FIG. 2. (a) Initiation time, (b) initiation month, (c) storm type, (d) initiation location with respect to a surface boundary, (e) initiation location (each box is 1° latitude by 1° longitude), (f) distance from a surface boundary for CS CI mode events, (g) severe-storm type, and (h) LLJ criterion (a criterion-0 LLJ represents no LLJ signature) for all events from 1996 to 2015.

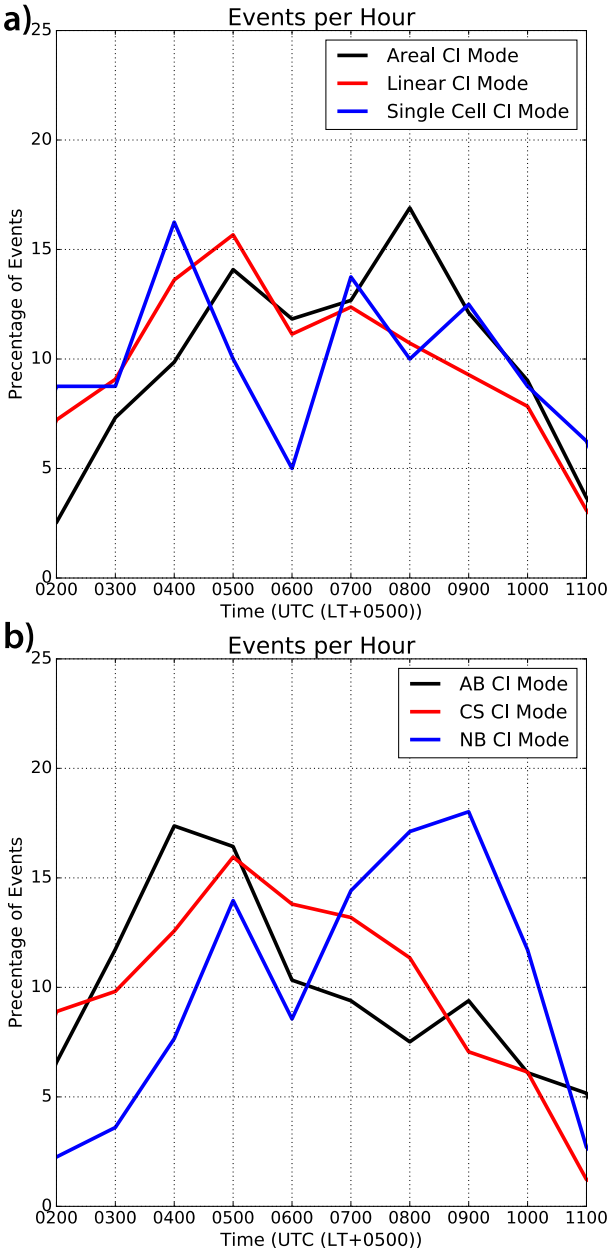

FIG. 3. Initiation time for (a) areal, linear, and single-cell storm type CI modes and (b) AB, CS, and NB CI modes. The reader should be cautious not to compare (a) to (b) because only each panel contains independent cases.

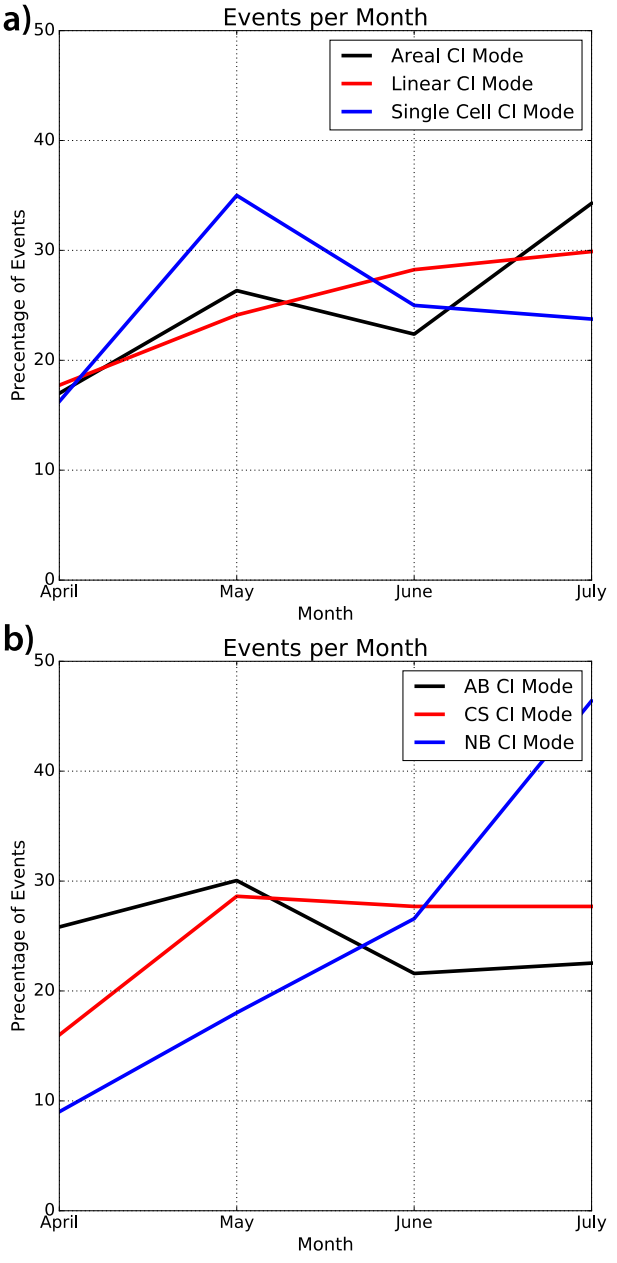

FIG. 4. Initiation month for (a) areal, linear, and single-cell storm type CI modes and (b) AB, CS, and NB CI modes.

events is early during the night while the peak initiation time for the areal storm-type CI mode events and the NB CI mode events is later during the night (Fig. 3). Perhaps the most important difference among the modes is the later initiation time of the NB CI mode events than the initiation time of the AB and CS CI mode events (cf. 0900 UTC to 0400 and 0500 UTC, respectively). A hypothesis for this later initiation time will be discussed in a later section.

b. *Initiation month*[6]

The most common initiation month varies among the six CI modes (Fig. 4), but there are notable patterns.

[6] Note that August was not initially considered for this study, but it is hypothesized that the climatology for August would be similar to that of July (Riley et al. 1987).

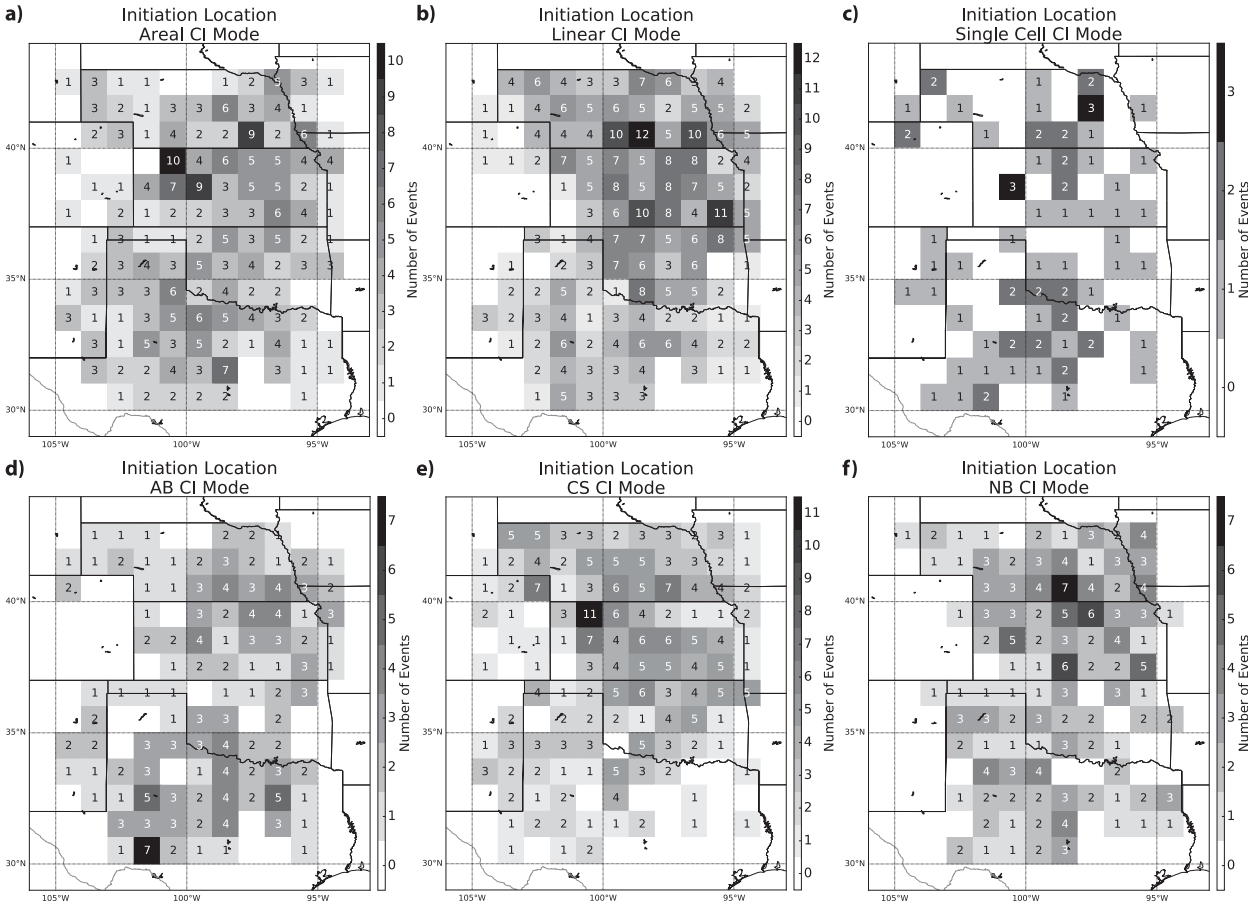

FIG. 5. Initiation location (each box is 1° latitude by 1° longitude) for (a) areal storm type, (b) linear storm type, (c) single-cell storm type, (d) AB CI mode, (e) CS CI mode, and (f) NB CI mode. The color scales are different to emphasize the differences in initiation location among the six modes.

The most common initiation month of the single-cell storm-type CI mode events and the AB CI mode events is May and the number of events in each month decreases as the warm season progresses. Conversely, the most common initiation month for the areal storm-type CI mode events and the NB CI mode events is July and the number of events per month increases as the warm season progresses. There is no peak initiation month for the CS CI mode.

c. *Initiation location*

The preferred initiation location is in the northern half of the domain for all CI modes except for the single-cell storm-type CI mode and the AB CI mode, for which the preferred initiation location is in the southern half of the domain (Fig. 5). Recall that there were two preferred initiation locations: the primary one in the northern half of the domain and the secondary one in the southern half of the domain. The primary initiation location is due mainly to the CS CI mode events and NB CI mode events, while the secondary initiation location is due mainly to the AB CI mode events. The primary initiation location of AB CI mode events is in Texas and the secondary initiation location is in northeastern Kansas. These different locations are associated with different types of surface boundaries. The events in Texas form on drylines and cold fronts, while the events in northeastern Kansas form on quasi-stationary fronts and cold fronts (not shown). It is surprising that the NB CI mode events have a distinct initiation location (south-central Nebraska and north-central Kansas). Without any strong surface forcing, why is there a clear initiation location? This question is addressed in the following sections.

d. *Linear system orientation*

As a whole, the linear systems do not have any preferred orientation, but the linear systems in the AB CI mode, the CS CI mode, and the NB CI mode do have

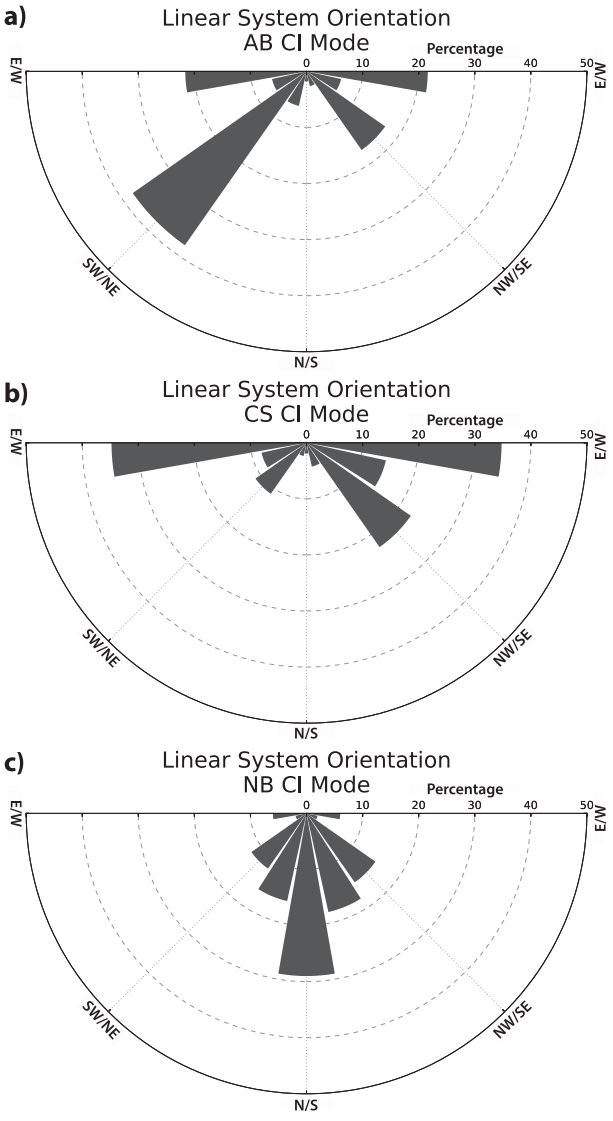

FIG. 6. Linear system orientation for the (a) AB CI mode, (b) CS CI mode, and (c) NB CI mode.

preferred orientations (Fig. 6). The linear AB CI mode events and the linear CS CI mode events are oriented southwest–northeast and east–west, respectively. It is notable that the linear NB CI mode events have a north–south orientation, even though there is no north–south-oriented surface boundary (or any surface boundary at all). Possible reasons for this finding will be discussed in later sections.

e. Initiation relative to surface boundaries

Fewer areal storm-type CI mode events initiate on a surface boundary than those that initiate on the cold side of a surface boundary or those that initiate with no nearby surface boundary (Fig. 7a). The preferred initiation location is on the cold side of a surface boundary for events in the linear storm-type mode (Fig. 7b) and along a surface boundary for single-cell storm-type CI mode events (Fig. 7c). The linear storm type being the preferred storm type on the cold side of a surface boundary (Fig. 7e) could be related to the widespread conditions (the broad areal extent of the LLJ and of moisture advected up and over a quasi-stationary front) that affect convection, as well as the continuous forcing from the LLJ during the night. A higher percentage of single-cell storm-type CI mode events begin on surface boundaries than those that begin on the cold side of a surface boundary or those that begin without a nearby surface boundary (Figs. 7d,e). There are many drylines and slow-moving cold fronts that accompany these events, both of which could favor discrete initiation.

f. Representative wind profile analysis

The wind directions at 500 hPa, 850 hPa, and the surface were taken from the representative soundings and examined to identify differences among the six CI modes. For all modes of CI except for the NB CI mode, the 500-hPa flow is westerly (Fig. 8). However, the spread is higher for the storm-type modes than for the AB CI mode and the CS CI mode, probably because the latter two CI modes occur when there is a more characteristic synoptic-scale setup than when the storm type modes occur. For example, an areal storm can form when there are many different types of synoptic-scale patterns, but quasi-stationary fronts over the plains occur when there are relatively fewer types of synoptic-scale patterns (a typical location for corridors of high precipitation total during the warm season is north of an upper-level cyclone under a strong gradient in the westerly flow; Tuttle and Davis 2006). It is noteworthy that even though the NB CI mode events do not have a preferred 500-hPa wind direction, the 850-hPa wind direction is southerly to southwesterly.[7] The areal and linear CI modes may exhibit a preferred 850-hPa wind direction, but the variation is larger than that of the NB CI mode 850-hPa wind direction. The southerly or southwesterly wind at 850 hPa for NB CI mode events may indicate that the LLJ has a more important role in this CI mode than the others, but that role is not yet clear.

[7] Wind profiler data were examined to identify possible differences between the 0600 and 1200 UTC wind direction. There were not any major differences in the wind direction as the difference was usually less than 25°.

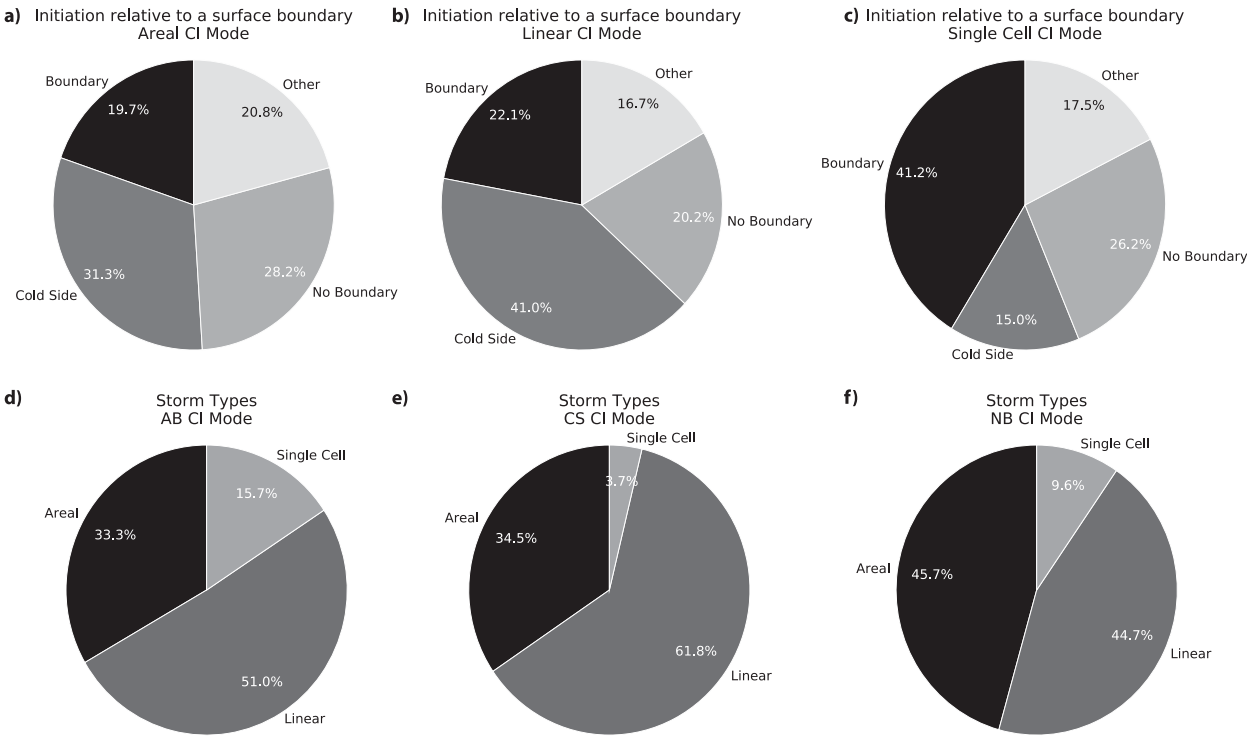

FIG. 7. Initiation location with respect to a surface boundary for the (a) areal storm-type CI mode, (b) linear storm-type CI mode, and (c) single-cell storm-type CI mode. Storm types for the (d) AB CI mode, (e) CS CI mode, and (f) NB CI mode.

The most common surface wind direction for nocturnal CI modes is southerly (Fig. 9). The exceptions are the AB CI mode events where there is no dominant surface wind direction and the CS CI mode events where the surface wind direction ranges from northerly to easterly to southerly. The events in the AB CI mode events have a wide range of surface boundaries, including drylines, warm fronts, cold fronts, quasi-stationary fronts, and outflow boundaries. These different boundaries will have slightly different surface wind directions, so there should not be a dominant surface wind direction. The surface wind direction tends to be easterly on the cold side of a quasi-stationary front and northerly to northwesterly on the cold side of a cold front.

It is noteworthy that the surface wind direction for NB CI mode events is southerly. The prevailing winds over the Great Plains are southerly, so this may be reflective of the typical, weak synoptic-scale setup that characterizes these events.

g. *Severe events*

Overall, over half of the events in each mode are nonsevere (not shown). However, the linear storm-type CI mode, the AB CI mode, and the CS CI mode have the highest percentage of severe events. For all modes of CI, hail is the preferred severe type and accounts for 84% of all severe events (Fig. 10). Wind events (38.4% of all severe events) and flooding events (26.3% of all severe events) are the next two common.[8] Flooding events account for nearly 10% of all events in the areal and linear storm-type modes (Figs. 11a,b), as well as the AB and CS CI modes (Figs. 11d,e). The slightly higher percentage of flooding events for the CS CI mode corresponds well with studies by Maddox et al. (1979), Trier and Parsons (1993), Rochette and Moore (1996), and Moore et al. (2003).

1) HAIL

Since hail events account for 84% of all severe events, this analysis reflects that of the severe events as a whole. The peak initiation time is relatively early at night and the peak initiation month is May (Fig. 12). The primary initiation location is from western Kansas to south-central Nebraska and a secondary initiation location spans a region from just south of the Red River to southwestern Texas. These events occur mainly in linear systems and over 80% of events initiate on the cold side of a surface boundary or on a surface boundary (Fig. 12e).

There are 148 hail-only events (about 16% of all events and about 50% of severe-hail events). A notable difference between the hail-only events and the events

[8] Note that these percentages do not add up to 100% because many events included more than one type of severe report.

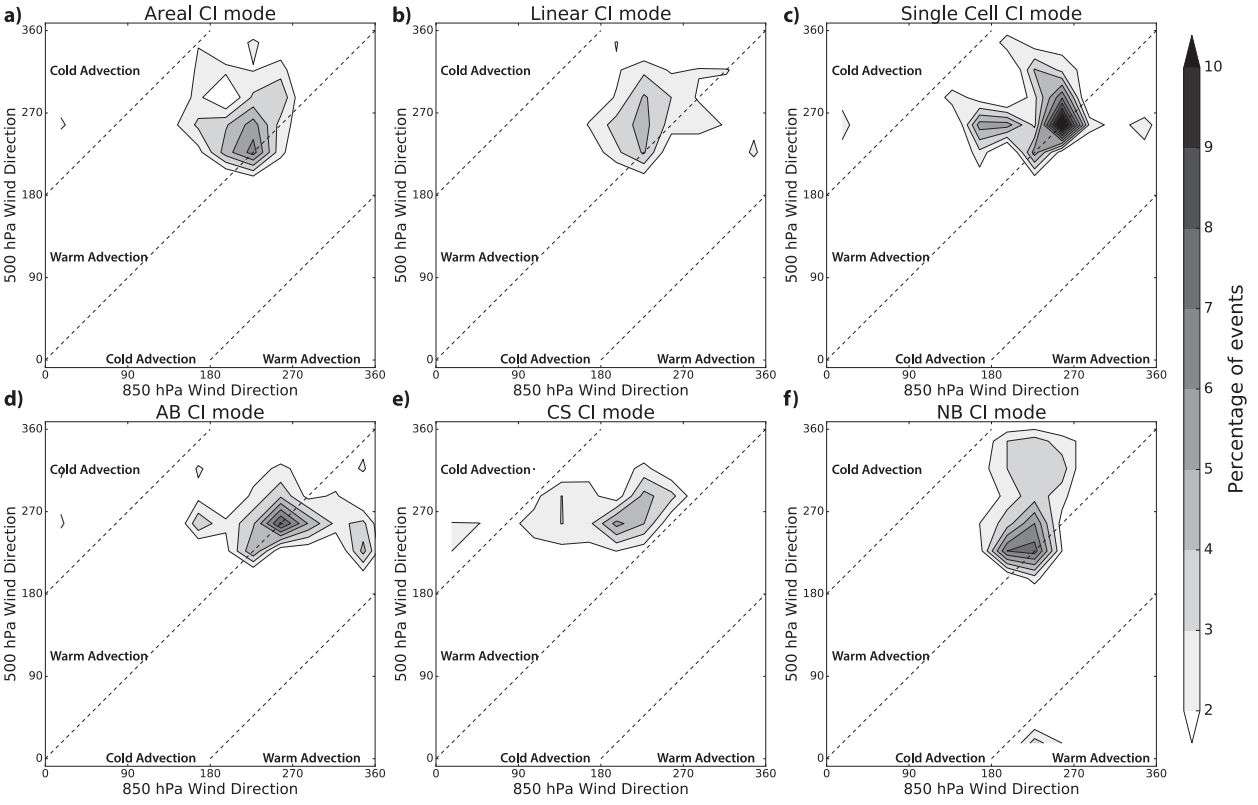

FIG. 8. 500-hPa wind direction (compass heading in degrees) vs 850-hPa wind direction taken from representative soundings for the (a) areal storm-type CI mode, (b) linear storm-type CI mode, (c) single-cell storm-type CI mode, (d) AB CI mode, (e) CS CI mode, and (f) NB CI mode. Warm and cold advection are labeled based on the veering and backing wind direction with height.

with hail and at least one other type of severe report is that there is no peak initiation time for the hail-only events (Fig. 12f). The initiation location for the hail-only events is also slightly different; there is a broad peak initiation location from northern Oklahoma to central Nebraska.

2) WIND

The most common initiation time for wind events is early at night and the most common initiation month is June (Fig. 13). There is no preferred initiation location for these events and the primary storm type for these events is linear (nearly 70% of the events). Like the hail events, over 80% of events are initiated on the cold side of a surface boundary or along a surface boundary; however, the number of cases for each is nearly equal (Fig. 13e).

There are only 19 wind-only events in the climatology. This is not surprising since the near-surface, nocturnal stable layer should limit the potential for severe winds to reach the surface. Since the sample size is small, it is hard to draw firm conclusions, but there are still some potentially significant findings. The peak initiation months are June and July (which account for almost 90% of the events), the peak initiation time is 0700 UTC, and there is a secondary peak initiation at 0400 UTC. The primary initiation location of wind-only events is western Nebraska and a relatively high percentage of these events begin on a surface boundary (Fig. 13f) compared to the percentage of events that are associated with severe reports other than just wind reports (Fig. 13e). Nearly 90% of these wind-only events occur with a LLJ and most often occur later during the night (not shown). Horgan et al. (2007) suggested that wind-only events are characterized by relatively shallow stable layers and lower CAPE than those for events that produce other severe reports. The percentage of events that occur on the cold side of a surface boundary is lower than that of those that have more than just high-wind reports, suggesting that the events that produce severe reports other than just winds are associated with stronger near-surface stable layers (Fig. 13e). Events that form on the cold side of a surface boundary typically have stronger near-surface stable layers and higher most-unstable CAPE. If there is a weak stable layer, then momentum associated with the LLJ could be mixed down to the surface more easily.

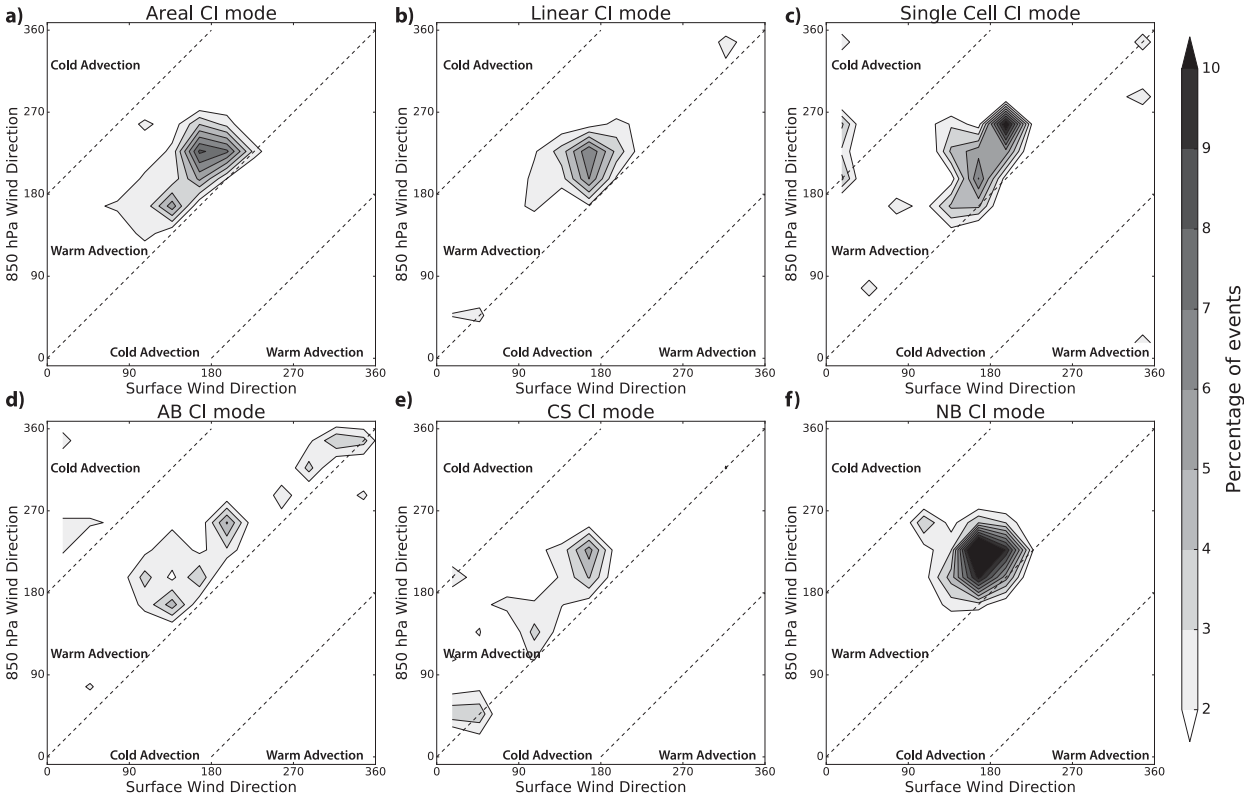

FIG. 9. As in Fig. 8, but for the 850-hPa wind direction (compass heading in degrees) vs surface wind direction taken from representative soundings.

3) FLOODING

The most common initiation time for flooding events is early at night and the most common initiation month is May, which accounts for nearly half of the events (Fig. 14). There is no preferred initiation location, but there is a broad maximum in eastern Kansas and a broad secondary maximum in central Texas. These events are primarily associated with linear convective systems and there are much fewer single cells for this severe type than for the other two severe types. Over half of these events occur on the cold side of a surface boundary (Fig. 14e; corresponding well with Maddox et al. 1979) and tend to occur in regions of low-level warm advection (not shown), corresponding well with Moore et al. (2003). Flooding is also common on the cold side of quasi-stationary fronts where convective echoes train over the same area (Schumacher and Johnson 2005).

The most common initiation month of the 33 flood-only events is June and while there is no peak initiation time, the majority of the events occur before 0800 UTC (not shown). The primary initiation location is in eastern Kansas and there is a secondary maximum in central Texas, like the events with more than only a flood report. Nearly 60% of these events are associated with the areal storm type (Fig. 14f). It is possible that there are more areal events that have only flood reports owing to the areal extent of the convection.

h. LLJ and non-LLJ events

The southerly nocturnal LLJ is common in all six modes of CI, but the single-cell storm-type mode events and the AB CI mode events have a lower percentage of LLJs than the other CI modes (Fig. 15). It is likely that the percentage is lower because the AB CI mode events may not need the extra forcing associated with an LLJ in order for CI to occur (for the AB mode events, ascent at the convergent surface boundary may be enough to lift air parcels to the LFC). It may be important that the NB CI mode events have the highest percentage of criterion-4 LLJs; this finding may mean that the LLJ is more important in generating convection for this mode than for the others.

Events associated with an LLJ most often are initiated north of the approximate LLJ center (Fig. 16). However, neither the NB CI mode events nor the single-cell events have a preferred initiation location north or south of the LLJ, but nearly 75% of the NB CI mode events initiate on

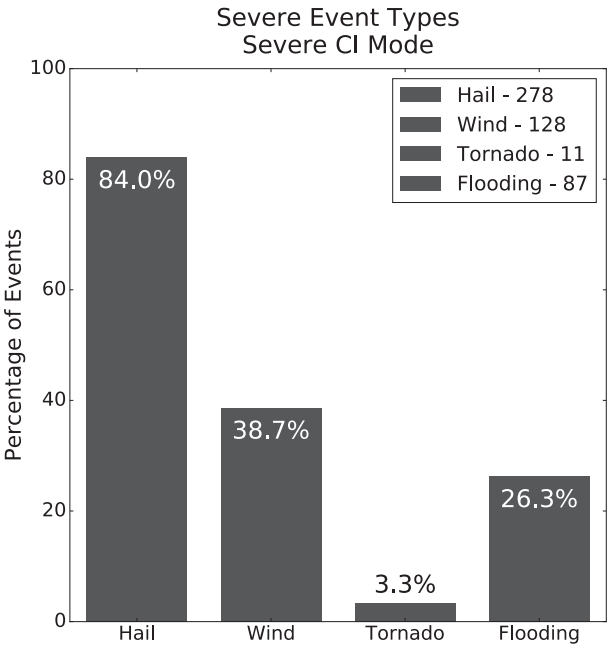

FIG. 10. Percentage of each type of severe-only events.

the eastern (anticyclonic shear) side of the approximate LLJ center. Similar results have been shown by Pu and Dickinson (2014). Relatively weak vorticity advection aloft such that vorticity advection becomes more cyclonic with height on the anticyclonic-shear side of and downstream from the jet favors quasigeostrophic (QG) ascent (Bluestein 1993) on the north and east side of the LLJ (Bluestein 1993).

4. Discussion

In the 20-yr climatology, nocturnal CI events over the central and southern Great Plains during the warm season tend to occur relatively early at night and in north-central Kansas and south-central Nebraska. These events are mostly nonsevere and occur with an LLJ in the domain. The most notable differences are among the AB CI mode, the CS CI mode, and the NB CI mode.

The peak initiation time is early at night for the AB CI mode events and the CS CI mode events, and later at night for the NB CI mode events. Shapiro et al. (2016) presented a theory for the development of the LLJ that combines the Blackadar (1957) and Holton (1967) theories and showed that the peak LLJ intensity occurs a few hours before sunrise. When the LLJ is at its peak intensity, convergence and cyclonic differential vorticity advection are strongest, resulting in the strongest LLJ-related ascent. Since the NB CI mode events typically occur with a LLJ (and in many cases, a strong LLJ), then this may be one factor that promotes initiation and may be one reason for the later initiation time of these events.

Prior convection near the Rocky Mountains also may be important. The distance from central Colorado to central Nebraska is approximately 600 km. If the air flows at $15\,m\,s^{-1}$ it takes nearly 11 h to traverse that distance. If the prior convection initiated at 2100 UTC (a common time according to Carbone et al. (2002) and Carbone and Tuttle (2008)), then moisture from the convection could reach central Nebraska between 0800 and 0900 UTC. This advection of moisture from prior convection is just one hypothesis for the relatively late initiation time of the NB CI mode.

The mountain–plains solenoidal circulation (Tripoli and Cotton 1989; Wolyn and McKee 1994; Carbone and Tuttle 2008) develops during the day and is characterized by an ascending branch over the Continental Divide and a descending branch over much of the Great Plains. At night, this circulation reverses sign (Carbone and Tuttle 2008; Sun and Zhang 2012) and the Great Plains is characterized by broad ascent (Carbone and Tuttle 2008, see their Fig. 9). They attribute this reversal to the differential cooling rates of the mountains and the plains. If the reversal is related to the differential cooling rates, then as the night progresses, the circulation should strengthen and ascent should increase throughout the night. This may be one factor in the later initiation time of the NB CI mode events; however, there is still uncertainty as to how far from the Rocky Mountains the effect of the solenoidal circulation is felt (Wolyn and McKee 1994; Carbone and Tuttle 2008).

The most common initiation month for AB CI mode events is May, there is no peak initiation month for CS CI mode events, and the most common initiation month for NB CI mode events is July. This finding may reflect the transition between stronger synoptic forcing and weaker synoptic forcing that occurs during late spring and early summer over the Great Plains. The relatively higher percentage of NB CI mode events during the summer months may imply weaker synoptic-scale forcing (fewer surface boundaries to initiate storms on or on the cold side of) and the relatively higher percentage of AB CI mode events and CS CI mode events in the late spring months may imply stronger synoptic-scale forcing.

The most common initiation location is in the southern half of the domain for AB CI mode events and is in the northern half of the domain for CS CI mode events and NB CI mode events. Early in the warm season, there are many dryline days and days with southward-moving cold fronts. Since drylines are mainly found in the southern half of the domain early in the warm season and cold fronts typically move from north to south, it is

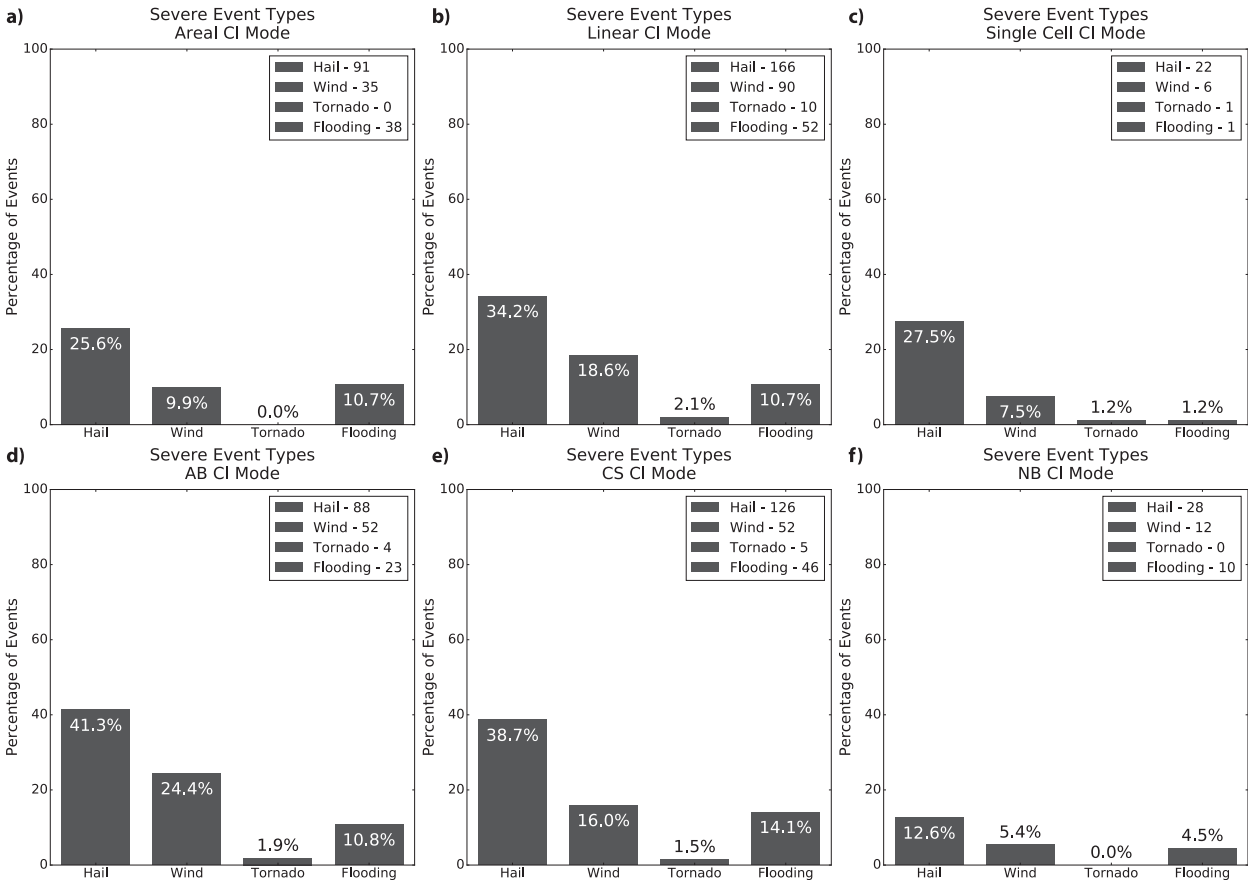

FIG. 11. Severe event type for (a) areal storm type, (b) linear storm type, (c) single-cell storm type, (d) AB CI mode, (e) CS CI mode, and (f) NB CI mode.

not surprising that the AB CI mode is reflective of this. The initiation location for the CS CI mode events has been explained by many previous studies (e.g., Maddox et al. 1979; Trier and Parsons 1993). Air flows up and over a quasi-stationary front, placing the initiation location farther north than the location of the AB CI mode events. One possible reason as to why the initiation location for the NB CI mode events is in the northern half of the domain is that it is approximately the location where the moisture advected eastward aloft from the prior convection to the west and the strongest ascent related to the LLJ overlap.

Approximately half of the AB CI mode events are severe, while a slightly lower percentage of the CS CI mode events are severe. There are two notable differences between the severe-type percentages for the two modes: the percentage of severe-wind events for AB CI mode events is higher than the percentage for CS CI mode events and the percentage of flooding events for AB CI mode events is lower than for CS CI mode events. Reasons for the relative lack of severe-wind reports for the CS CI mode events were proposed by Horgan et al. (2007). They suggested that the near-surface stable layer (implying a relative lack of mixing of higher momentum from aloft) limits the potential for severe winds to reach the surface. The near-surface stable layer is likely stronger on the cold side of a surface boundary than on the warm side of the surface boundary. The synoptic-scale setup is favorable for flooding events on the cold side of surface boundaries (Maddox et al. 1979; Fritsch et al. 1986; Trier and Parsons 1993), and the flooding events tend to occur south of an upper-level divergence maximum (Schumacher and Johnson 2005). The higher percentage of flood events associated with CS CI mode events is consistent with their studies.

Since the nocturnal LLJ is a common phenomenon over the Great Plains during the warm season, there is a high percentage of events associated with an LLJ. The percentage of the AB CI mode events that have an LLJ signature in the domain is less than that of the CS CI mode events and that of NB CI mode events, perhaps because the AB CI mode events do not require extra forcing associated with an LLJ in order to get CI. The percentage of events with an LLJ signature in the

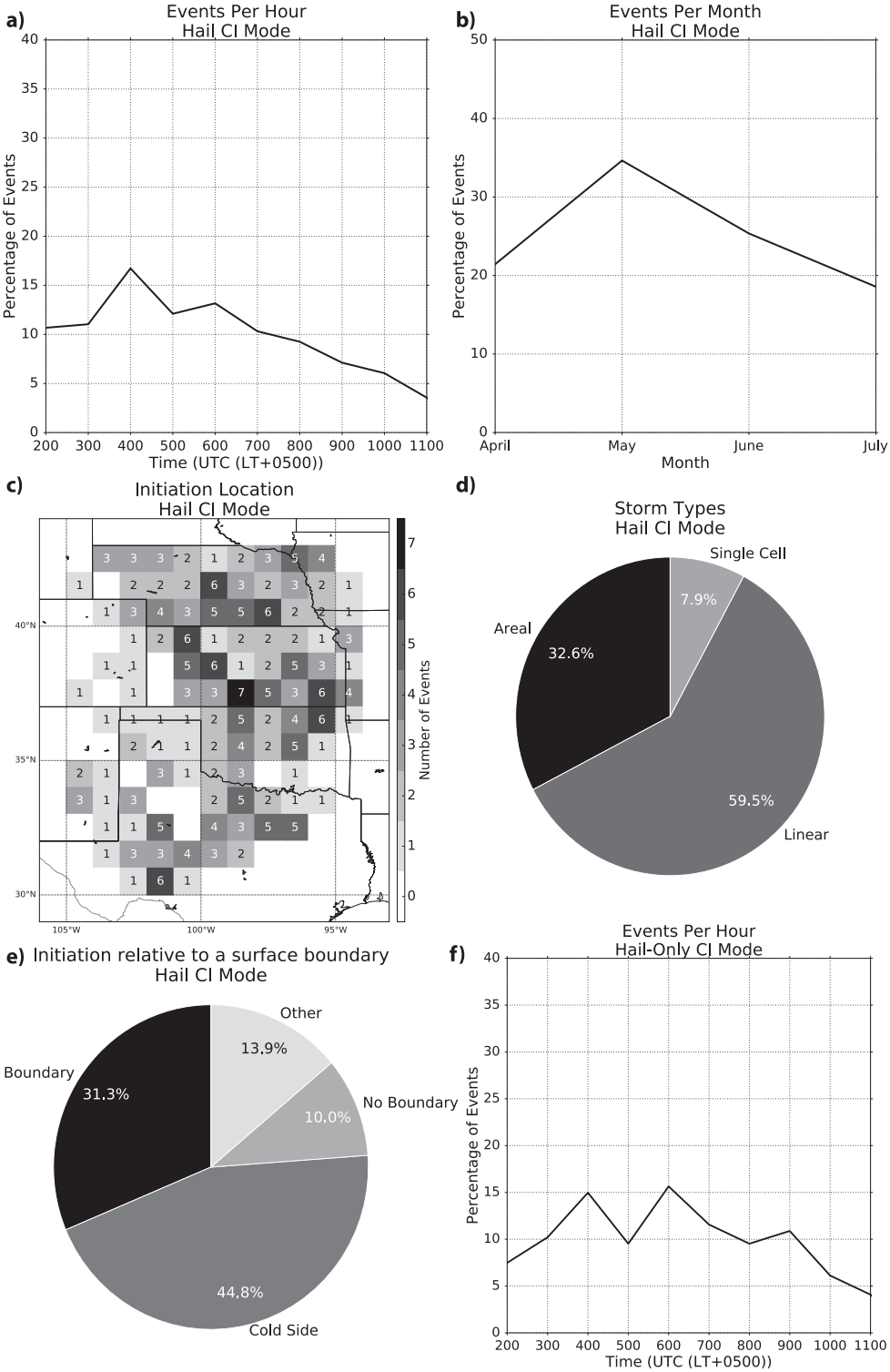

FIG. 12. (a) Initiation time, (b) initiation month, (c) initiation location, (d) storm type, (e) initiation location relative to a surface boundary for severe-hail events, and (f) initiation time for events that only produced severe-hail reports.

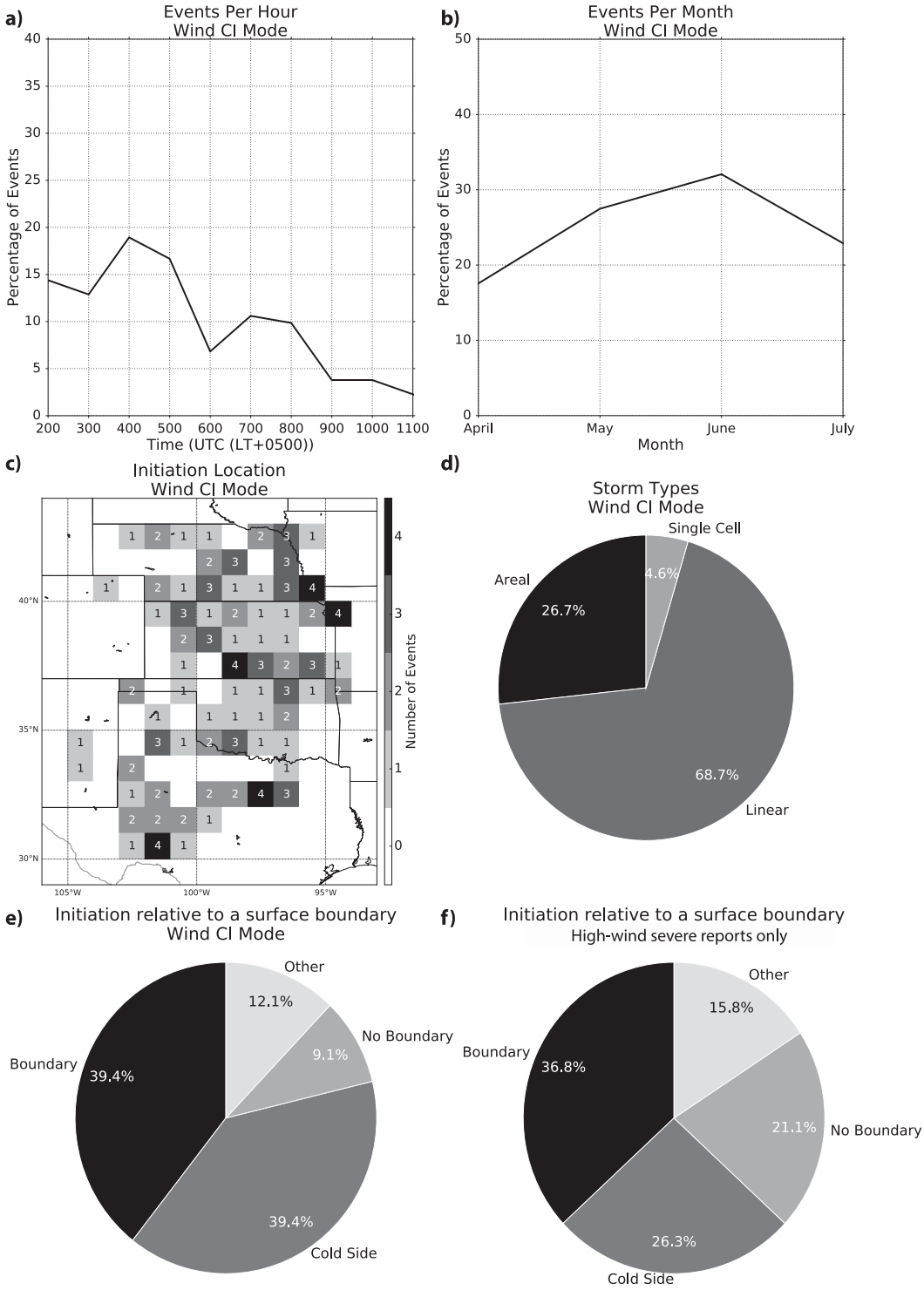

FIG. 13. (a) Initiation time, (b) initiation month, (c) initiation location, (d) storm type, (e) initiation location relative to a surface boundary for severe-wind events, and (f) initiation location relative to a surface boundary for events that only produced severe-wind reports.

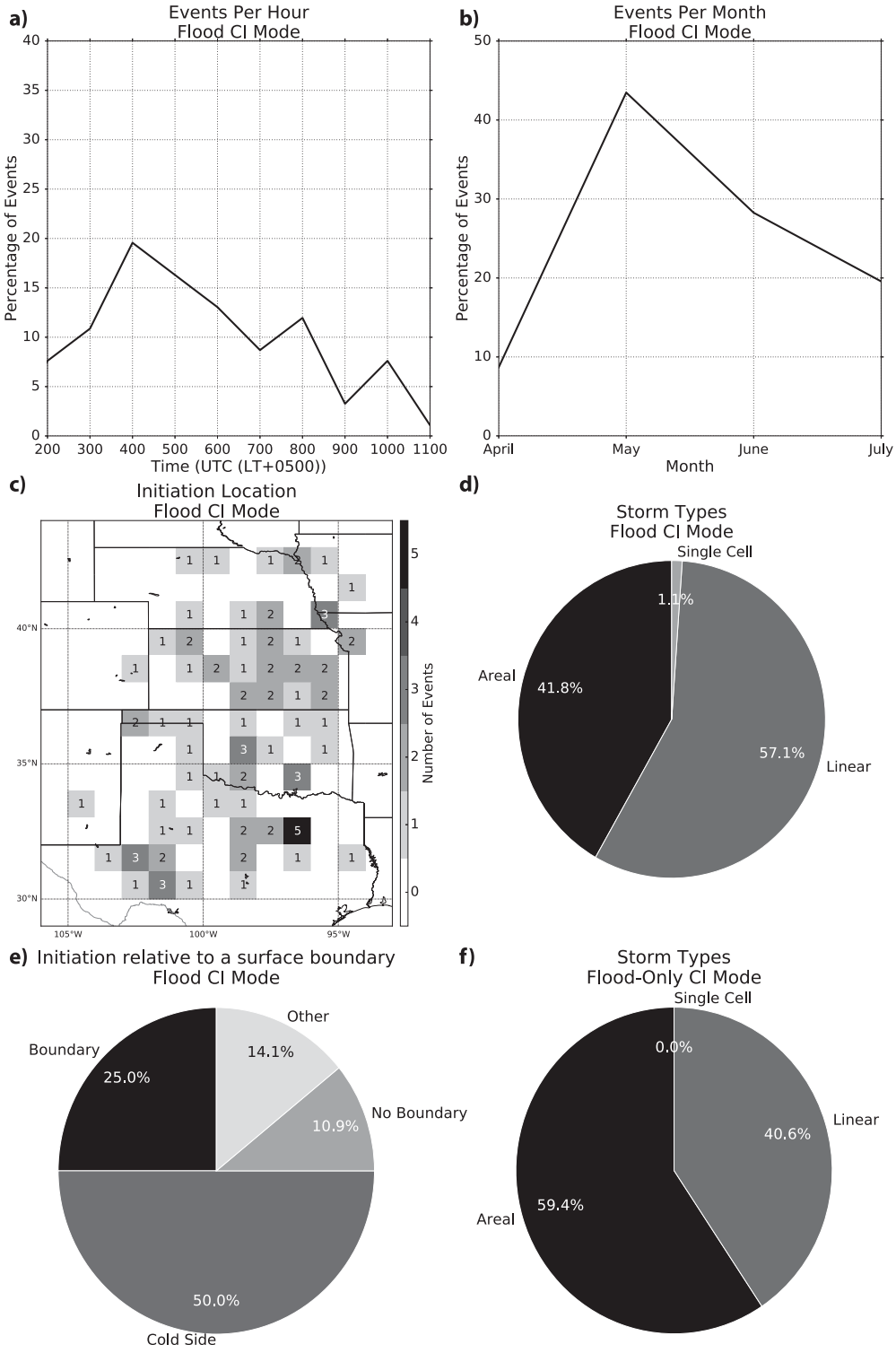

FIG. 14. (a) Initiation time, (b) initiation month, (c) initiation location, (d) storm type, (e) initiation location relative to a surface boundary for flood events, and (f) storm type for events that only produced flood reports.

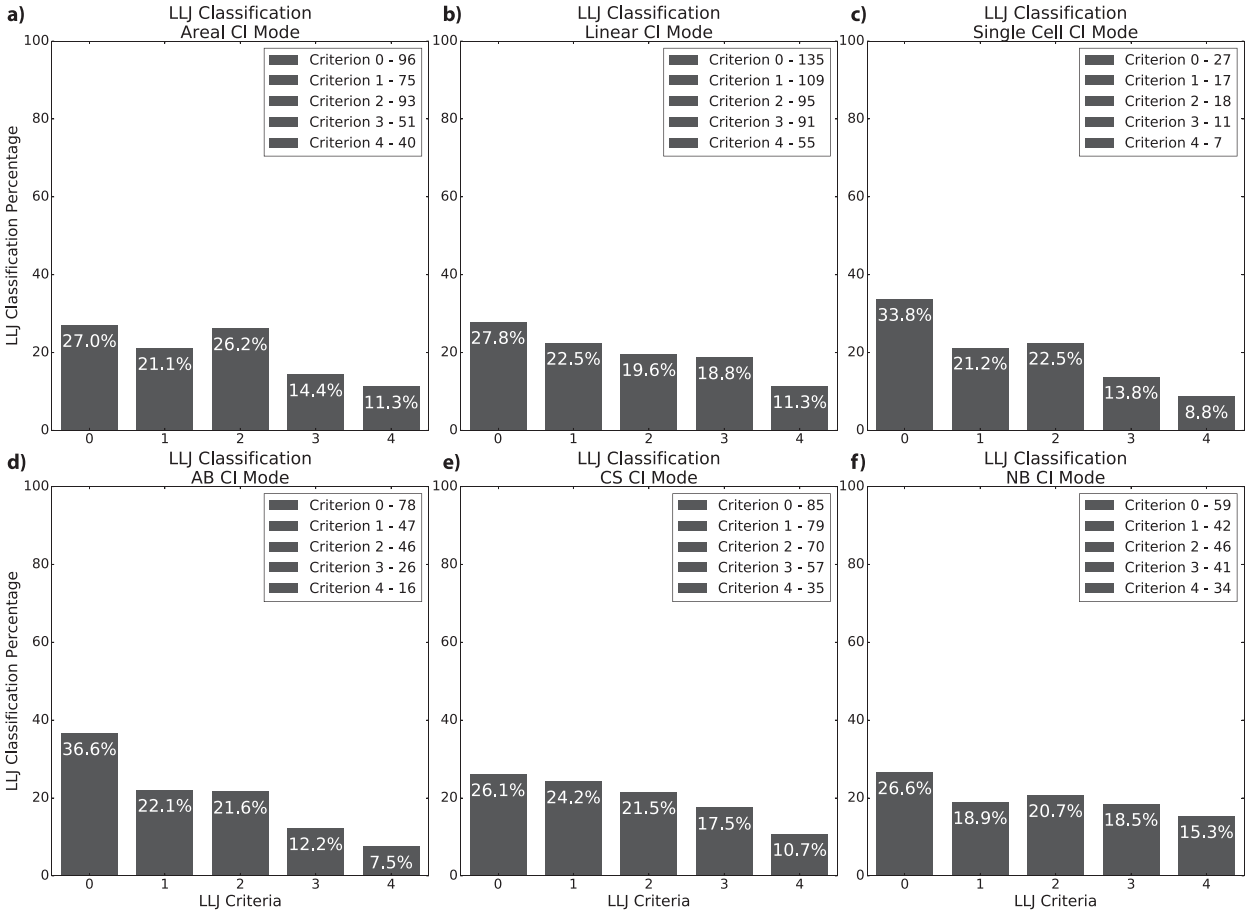

FIG. 15. Percentage of each criteria LLJ for (a) areal storm type, (b) linear storm type, (c) single-cell storm type, (d) AB CI mode, (e) CS CI mode, and (f) NB CI mode. Note that a "criterion 0" LLJ represents no LLJ signature in the domain.

domain is roughly the same for the CS CI mode events and the NB CI mode events. Recall that percentage of strong LLJs (criteria 3 and 4) is higher for the NB CI mode events than for the CS CI mode events, perhaps because the NB CI events need the extra forcing associated with a stronger LLJ than the CS CI mode events. For the CS CI mode events, the air goes up and over a surface boundary, so it already has a source of adequate lift even for weaker LLJs. The preferred initiation location for the NB CI mode events is the anticyclonic-shear side (eastern side) of the LLJ, unlike the preferred initiation location of the AB CI mode events and the CS CI mode events, whose preferred initiation location is north of the LLJ (though it not as far poleward for the AB CI mode events as it is for the CS CI mode events).

It has been shown that characteristics of the NB CI mode events are different from the characteristics of the events in the other two nocturnal CI modes (such as the north–south orientation of the linear systems and the later initiation time). A case study will be presented that represents a typical event in the NB CI mode to allow a closer look at possible initiation mechanisms that may not appear in a climatology.

5. Case study—5 July 2015 (NB CI mode)

a. Analysis

On 5 July 2015 a typical NB CI mode synoptic-scale setup occurred during the Plains Elevated Convection at Night (PECAN; Geerts et al. 2017) field project; thus, higher spatial resolution observations were available than if there had been no field project. There were three NB nocturnal CI events in Kansas on 5 July 2015. The first occurred in western Kansas at 0330 UTC, the second occurred north of the first event in northwestern Kansas at 0630 UTC, and the third occurred in east-central Kansas at 1100 UTC (Fig. 17). At 300 hPa there was a ridge over the Rockies and northwesterly flow over Kansas (Fig. 18a). At 700 hPa, there was westerly flow over western Kansas and warm advection over the CI

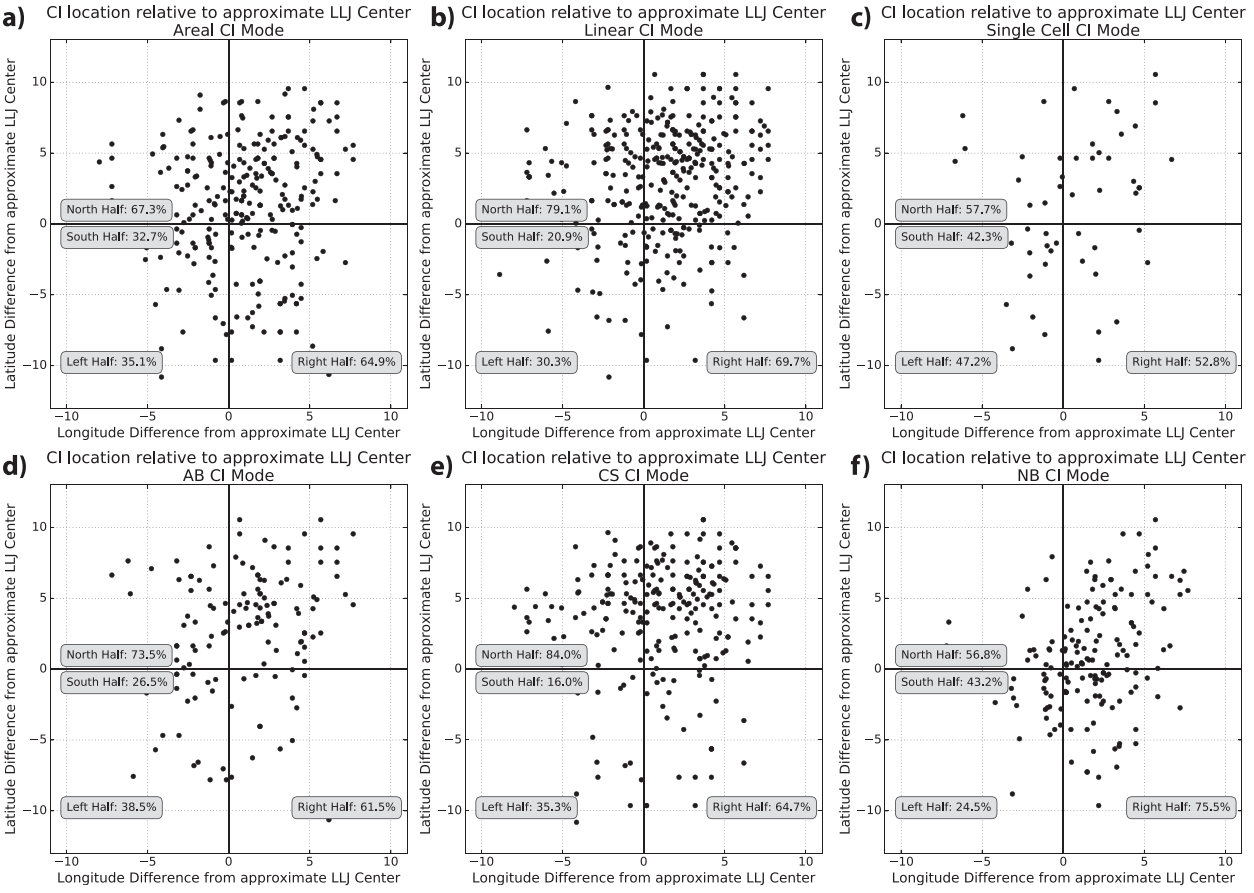

FIG. 16. Initiation location relative to the approximate LLJ center for (a) areal storm type, (b) linear storm type, (c) single-cell storm type, (d) AB CI mode, (e) CS CI mode, and (f) NB CI mode.

locations (Fig. 18b). There was a criterion-3 LLJ (not shown) and the CI occurred just east of the 850-hPa wind maximum (Fig. 18c), consistent with the results shown in section 3h. Since there was no surface wind shift or strong temperature or moisture gradients in Kansas or Nebraska, there was no nearby surface boundary (Fig. 18d).

It is seen in the early evening visible satellite (not shown) and infrared images that there were preexisting convective systems, one in South Dakota at 0000 UTC and one in Nebraska by 0900 UTC (Figs. 19a,b). These convective systems, combined with the northwesterly mid- to upper-level flow over the region, allowed moisture from the systems to be advected into eastern Kansas prior to the third initiation event. Moisture was also advected from the earlier convection over the Rockies into western Kansas by the time of the first initiation event. In the water vapor satellite images, there was an area of drier air between the first CI event and the second CI event farther east (Figs. 19c,d; the arrow in Fig. 19c denotes the drier air). Precipitable water was high throughout the night and was in excess of 1.3 in. (33 mm) near the CI locations (Fig. 19e). Funk (1991) concluded that precipitable water values of greater than 1 in. (25.4 mm) are supportive of heavy rainfall.

The 0000 UTC KLBF (North Platte, Nebraska) sounding represented the area where the moisture originated (Fig. 20a). There was an area of higher moisture in a shallow layer at 600 hPa. This moisture was then advected southeastward into Kansas (as seen on the satellite images). There was warm advection (indicated by the low-level veering wind profile) at 0000 UTC as well as in the GFS analysis at 700 hPa between 0000 UTC and past the time of CI. Thus, the strongest area of QG ascent based on temperature advection probably occurred between 700 and 600 hPa.

During the PECAN project, a fixed-site sounding station was located in Ellis, Kansas, near where the first CI occurred and soundings were launched at 0000, 0300, and 0600 UTC (Fig. 20b; 0000 and 0300 UTC not shown). There was a shallow layer of moisture between 600 and 500 hPa in all three soundings and the most-unstable CAPE was greater than 1500 J kg^{-1} and the most-unstable CIN was relatively low (magnitude less than 125 J kg^{-1}). It will be shown in the second part of this

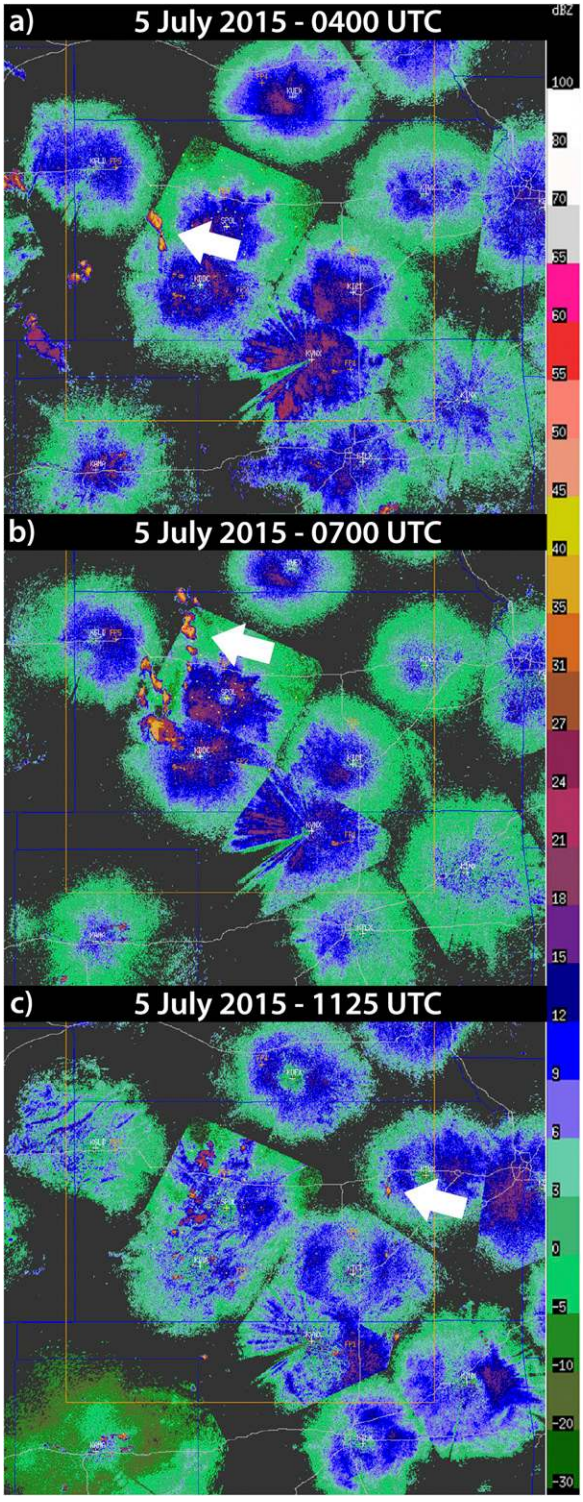

FIG. 17. Radar composites of the three CI events in Kansas on 5 Jul 2015. The white arrows denote CI locations.

study that a shallow layer of moisture is present in many NB CI mode events and may be an important parameter.

It is seen in an east–west-oriented cross section through 38°N that there was a midlevel moisture maximum (a layer of relative humidity greater than 70%) that extended from 800 to 600 hPa at 0000 UTC (Fig. 20c) and a moisture maximum that extended from the surface to 600 hPa at 0600 UTC. The strongest ascent is at 700 hPa in the model data, suggestive of the triggering of elevated convection (Fig. 20d). However, based on observations from the Ellis sounding, the ascent likely occurred higher in the atmosphere (near 600 hPa) because that is where the air is moistest (and MUCAPE is highest).

There was strong warm advection near 700 hPa, but differential vorticity advection was weak (Figs. 21a,b). Warm advection is associated with QG ascent and vorticity advection becoming more cyclonic with height is also associated with QG ascent. There are convergent **Q**-vectors in northern Oklahoma and central Kansas based on the GFS analysis at 700 hPa at 0600 UTC (Fig. 21c). Because the differential vorticity advection was weak (and negative, the opposite sign as temperature advection), warm advection near 700 hPa was the main contributor to QG ascent.

b. Conclusions from the case study

The case study presented an analysis of nocturnal convection that initiated with no nearby surface boundary, a CI mode that represents nearly 25% of all nocturnal CI and is most frequent in July. This is not the first analysis of this type of convection (see Bluestein 1985), but the number of case studies of this type of convection in the literature is low. The NB CI mode events have a few important characteristics: the shallow, elevated band of moisture, the warm advection between 800 and 600 hPa, the westerly flow over the Rockies (or at least a strong westerly component), and the nocturnal LLJ. These characteristics are not unique to this case study. The second part of this study will present more case studies to reinforce the importance of these features on CI as well as to add more case studies of an important, but relatively unstudied, mode of CI to the literature.

6. Summary

A 20-yr (1996–2015) climatology of nocturnal CI over the central and southern Great Plains was presented. Composite radar data were examined to identify any nocturnal CI over that region and surface data were examined to identify the initiation location with respect to any surface boundary. Two modes of CI relative to a surface boundary were identified: events that begin at a surface boundary and events that begin on

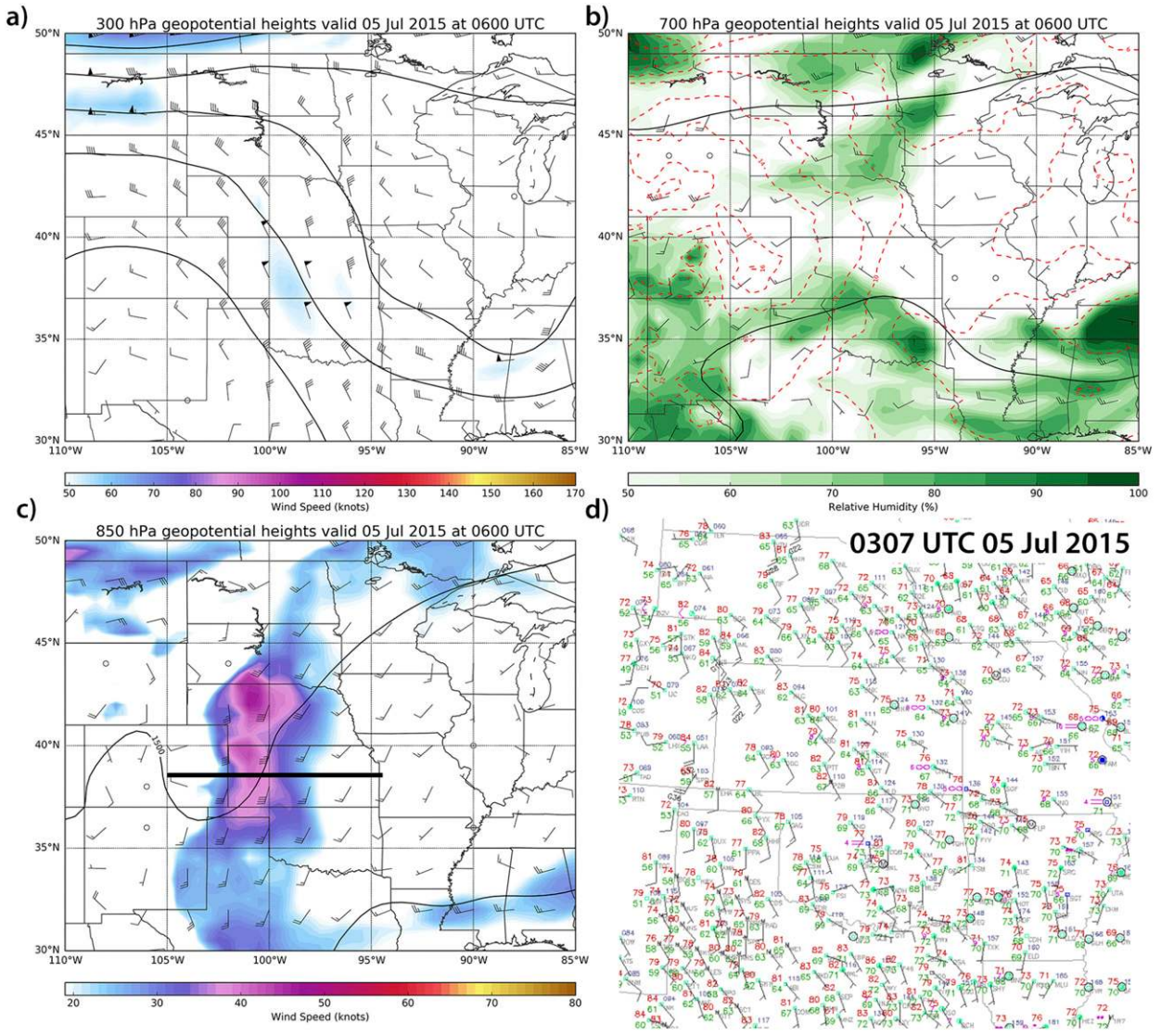

FIG. 18. GFS analysis valid at 0600 UTC 5 Jul 2015. (a) 300-hPa geopotential height and winds; (b) 700-hPa geopotential height, relative humidity, and winds; (c) 850-hPa geopotential height and winds; and (d) surface observations of pressure, temperature, and winds valid at 0307 UTC. A half barb represents 5 kt (2.5 m s^{-1}), a full barb represents 10 kt (5 m s^{-1}), and a flag represents 50 kt (25 m s^{-1}). The horizontal black line in (c) denotes the cross section in Fig. 20.

the cold side of a surface boundary. Events that begin with no nearby surface boundary represent another nocturnal CI mode.

The peak initiation location is in north-central Kansas and south-central Nebraska and the peak initiation time for AB CI mode events that initiate on a surface boundary and events that initiation on the cold side of a surface boundary is early at night. However, the peak initiation time of events that initiate with no nearby surface boundary is later at night (near 0900 UTC). These events, though are typically not as intense as events that initiate on a surface boundary and events that initiation on the cold side of a surface boundary. The AB CI mode, accounts for over 25% of all nocturnal convection and has unique characteristics, including a north–south orientation of the linear systems. A case study of an event that initiated with no nearby surface boundary was presented to identify possible important initiation features, some of which include the nocturnal LLJ, a midlevel moisture maximum, and midlevel warm advection. It is important to note that the evolution of the events in each CI mode was not documented. We plan to examine these characteristics in a future study.

Acknowledgments. The authors extend their thanks to Drs. Dave Parsons, Steven Cavallo, Lance Bosart,

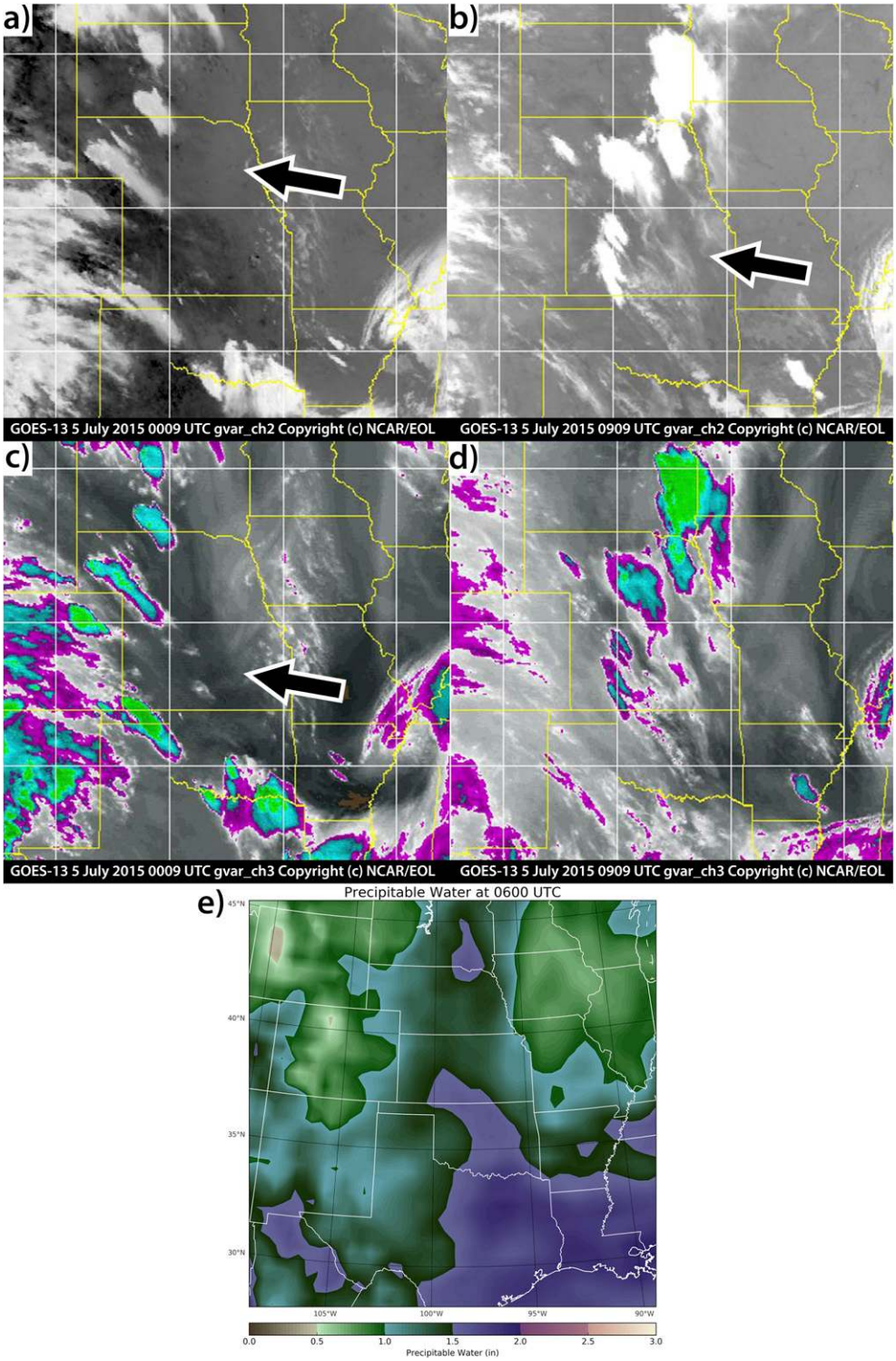

FIG. 19. *GOES-13* infrared satellite valid at (a) 0309 and (b) 0909 UTC and *GOES-13* water vapor imagery valid at (c) 0309 and (d) 0909 UTC. (e) Precipitable water (in.) from the GFS analysis valid at 0600 UTC. Arrows in (a) and (b) represent the moisture from the convective system in Nebraska that flowed over Kansas, and the arrow in (c) points out the drier air between the first and second CI events.

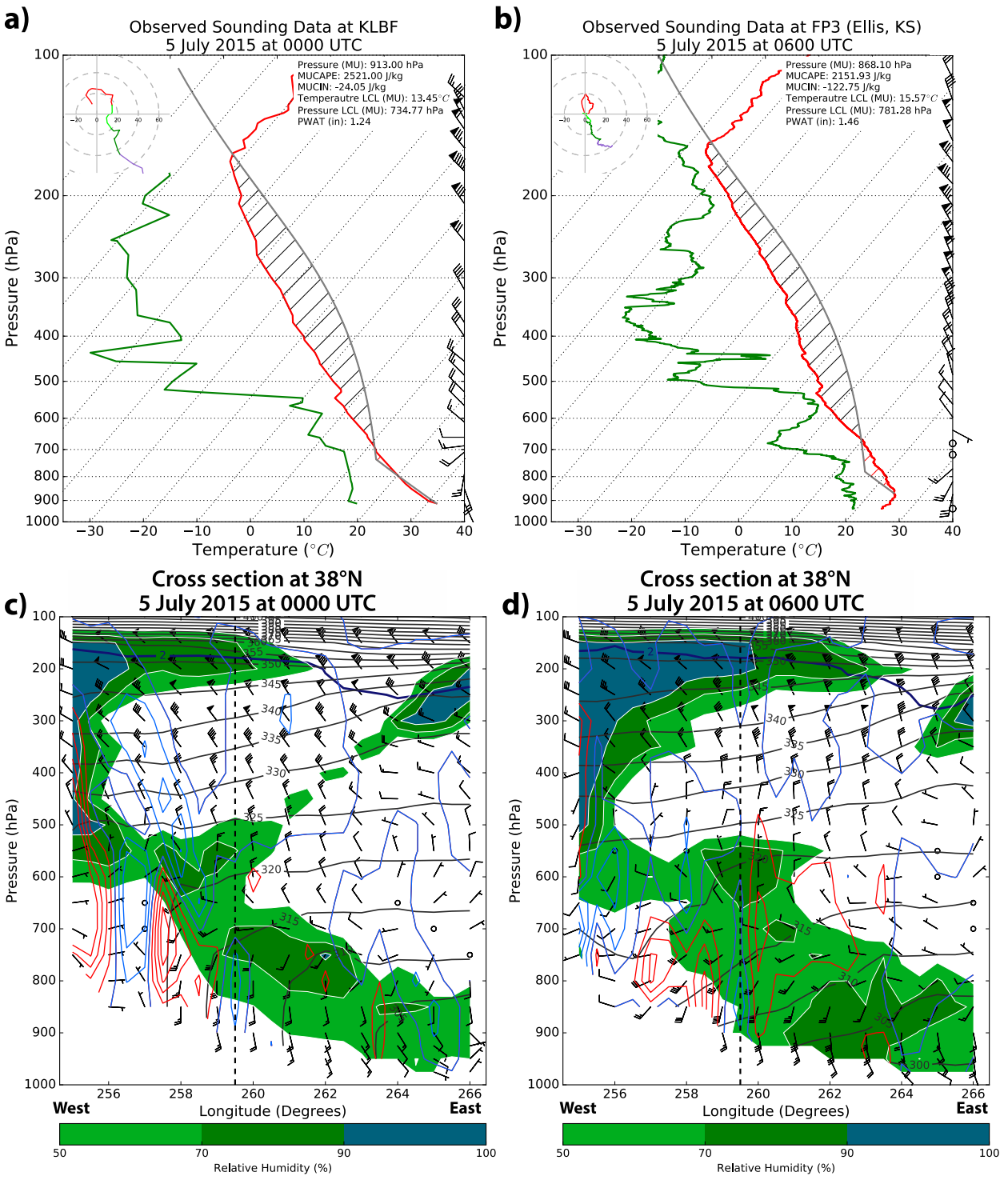

FIG. 20. Observed sounding data from (a) KLBF at 0000 UTC and (b) FP3 (Ellis, KS) PECAN sounding at 0600 UTC 5 Jul 2015. An east–west-oriented cross section using GFS data at 38°N valid at (c) 0000 and (d) 0600 UTC. The red and blue contours are ascent and descent (negative and positive omega), respectively. The dark gray contours are isentropes (intervals of 5 K), the green shaded regions are areas of relative humidity greater than 50%, and the vertical dashed line is roughly the location of CI. Wind barbs are as in Fig. 18.

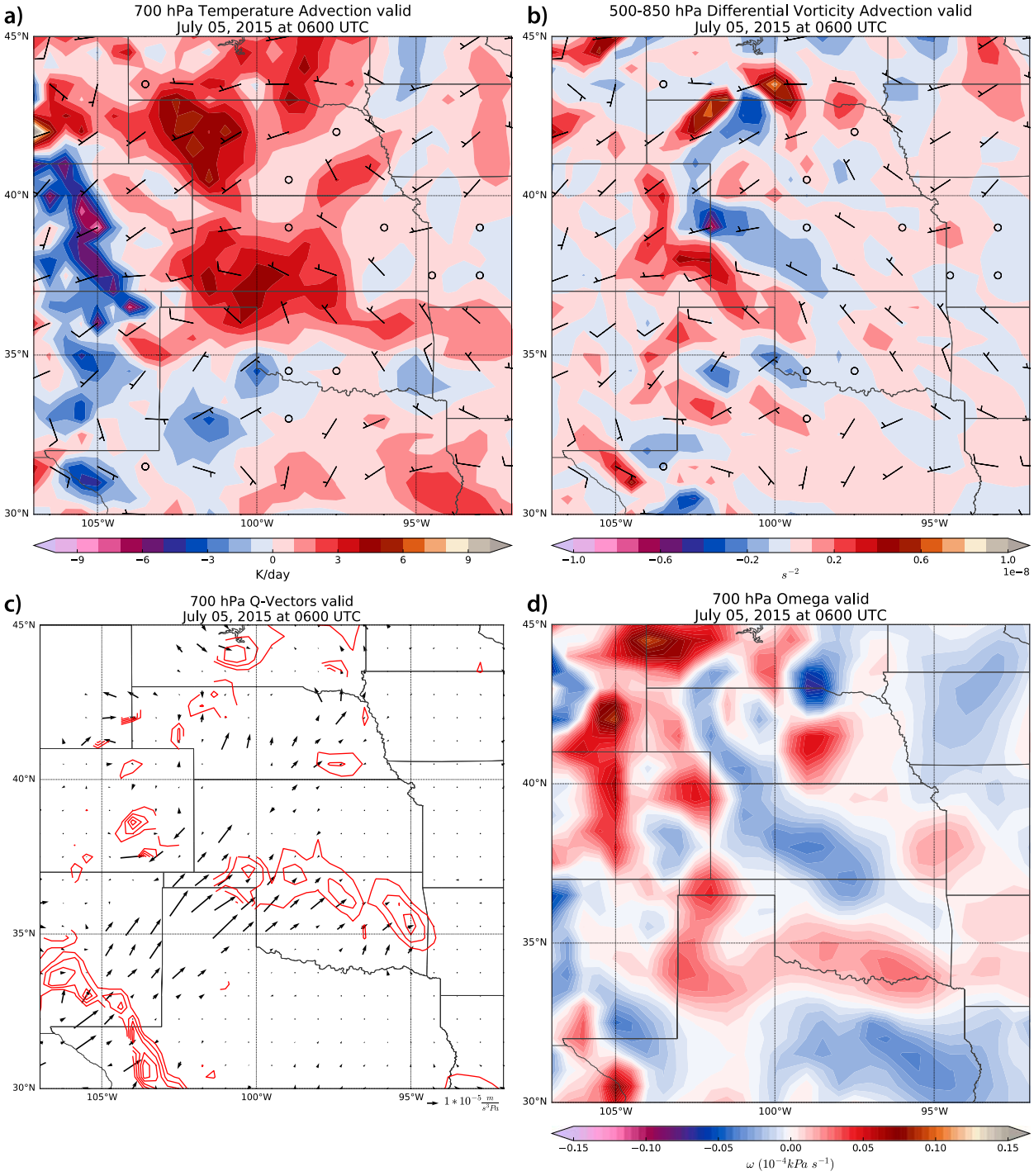

FIG. 21. (a) 700-hPa temperature advection and winds, (b) 500–850-hPa differential vorticity advection and 700-hPa winds, (c) 700-hPa **Q**-vectors and **Q**-vector convergence, and (d) omega taken from the GFS data valid at 0600 UTC. Wind barbs are as in Fig. 18.

Evgeni Fedorovich, and Alan Shapiro for all of their assistance and advice throughout the project, as well as Zach Wienhoff, Kyle Thiem, and Manda Chasteen for their advice and help. We also thank Dave Ahijevych at NCAR for obtaining missing images in the NCAR Image Archive and we thank Tammy Weckwerth for supplying the radar composite data used in the case study. We also acknowledge NSF Grants AGS-1237404 and AGS-1262048 for funding this research. PECAN data were provided by NCAR/EOL under sponsorship of the

National Science Foundation (available online at http://data.eol.ucar.edu/).

REFERENCES

Anderson, C. J., W. A. Gallus Jr., R. W. Arritt, and J. S. Kain, 2002: Impact of adjustments in the Kain-Fritsch convective scheme on QPF of elevated convection. Preprints, *19th Conf. on Weather Analysis and Forecasting*, San Antonio, TX, Amer. Meteor, Soc., 23–24.

Blackadar, A. K., 1957: Boundary layer wind maxima and their significance for the growth of nocturnal inversions. *Bull. Amer. Meteor. Soc.*, **38**, 283–290.

Bluestein, H. B., 1985: An observational study of a mesoscale area of convection under weak synoptic-scale forcing. *Mon. Wea. Rev.*, **113**, 520–538, doi:10.1175/1520-0493(1985)113<0520:AOSOAM>2.0.CO;2.

——, 1993: *Synoptic-Dynamic Meteorology in Midlatitudes.* Vol. I, *Principles of Kinematics and Dynamics*, Oxford University Press, 448 pp.

——, and M. H. Jain, 1985: Formation of mesoscale lines of precipitation: Severe squall lines in Oklahoma during the spring. *J. Atmos. Sci.*, **42**, 1711–1732, doi:10.1175/1520-0469(1985)042<1711:FOMLOP>2.0.CO;2.

Bonner, W. D., 1968: Climatology of the low level jet. *Mon. Wea. Rev.*, **96**, 833–850, doi:10.1175/1520-0493(1968)096<0833:COTLLJ>2.0.CO;2.

Carbone, R. E., and J. D. Tuttle, 2008: Rainfall occurrence in the U.S. warm season: The diurnal cycle. *J. Climate*, **21**, 4132–4146, doi:10.1175/2008JCLI2275.1.

——, ——, D. A. Ahijevych, and S. B. Trier, 2002: Inferences of predictability associated with warm season precipitation episodes. *J. Atmos. Sci.*, **59**, 2033–2056, doi:10.1175/1520-0469(2002)059<2033:IOPAWW>2.0.CO;2.

Colman, B. R., 1990a: Thunderstorms above frontal surfaces in environments without positive CAPE. Part I: A climatology. *Mon. Wea. Rev.*, **118**, 1103–1121, doi:10.1175/1520-0493(1990)118<1103:TAFSIE>2.0.CO;2.

——, 1990b: Thunderstorms above frontal surfaces in environments without positive CAPE. Part II: Organization and instability mechanisms. *Mon. Wea. Rev.*, **118**, 1123–1144, doi:10.1175/1520-0493(1990)118<1123:TAFSIE>2.0.CO;2.

Davis, C. A., K. W. Manning, R. E. Carbone, S. B. Trier, and J. D. Tuttle, 2003: Coherence of warm-season continental rainfall in numerical weather prediction models. *Mon. Wea. Rev.*, **131**, 2667–2679, doi:10.1175/1520-0493(2003)131<2667:COWCRI>2.0.CO;2.

Easterling, D. R., and P. J. Robinson, 1985: The diurnal variation of thunderstorm activity in the United States. *J. Climate Appl. Meteor.*, **24**, 1048–1058, doi:10.1175/1520-0450(1985)024<1048:TDVOTA>2.0.CO;2.

Fabry, F., 2012: Daily and annual cycles of precipitation and convection over the continental United States. *Proc. Seventh European Conf. on Radar in Meteorology and Hydrology*, Toulouse, France, Météo-France, 5 pp. [Available online at http://www.meteo.fr/cic/meetings/2012/ERAD/extended_abs/RCS_089_ext_abs.pdf.]

Fritsch, J. M., R. J. Kane, and C. R. Chelius, 1986: The contribution of mesoscale convective weather systems to the warm-season precipitation in the United States. *J. Climate Appl. Meteor.*, **25**, 1333–1345, doi:10.1175/1520-0450(1986)025<1333:TCOMCW>2.0.CO;2.

Funk, T. W., 1991: Forecasting techniques utilized by the forecast branch of the National Meteorological Center during a major convective rainfall event. *Wea. Forecasting*, **6**, 548–564, doi:10.1175/1520-0434(1991)006<0548:FTUBTF>2.0.CO;2.

Geerts, B., and Coauthors, 2017: The 2015 Plains Elevated Convection at Night (PECAN) field project. *Bull. Amer. Meteor. Soc.*, doi:10.1175/BAMS-D-15-00257.1, in press.

Grant, B. N., 1995: Elevated cold-sector severe thunderstorms: A preliminary study. *Natl. Wea. Dig.*, **19**, 25–31.

Holton, J. R., 1967: The diurnal boundary layer wind oscillation above sloping terrain. *Tellus*, **19**, 199–205, doi:10.1111/j.2153-3490.1967.tb01473.x.

Horgan, K. L., D. M. Schultz, J. E. Hales Jr., S. F. Corfidi, and R. H. Johns, 2007: A five-year climatology of elevated severe convective storms in the United States east of the Rocky Mountains. *Wea. Forecasting*, **22**, 1031–1044, doi:10.1175/WAF1032.1.

Kincer, J. B., 1916: Daytime and nighttime precipitation and their economic significance. *Mon. Wea. Rev.*, **44**, 628–633, doi:10.1175/1520-0493(1916)44<628:DANPAT>2.0.CO;2.

Maddox, R. A., 1980: Mesoscale convective complexes. *Bull. Amer. Meteor. Soc.*, **61**, 1374–1387, doi:10.1175/1520-0477(1980)061<1374:MCC>2.0.CO;2.

——, 1983: Large-scale meteorological conditions associated with midlatitude, mesoscale convective complexes. *Mon. Wea. Rev.*, **111**, 1475–1493, doi:10.1175/1520-0493(1983)111<1475:LSMCAW>2.0.CO;2.

——, C. F. Chappell, and L. R. Hoxit, 1979: Synoptic and meso-α scale aspects of flash flood events. *Bull. Amer. Meteor. Soc.*, **60**, 115–123, doi:10.1175/1520-0477-60.2.115.

Markowski, P., and Y. Richardson, 2010: *Mesoscale Meteorology in Midlatitudes*. Wiley-Blackwell, 424 pp.

Marsham, J. H., S. B. Trier, T. M. Weckwerth, and J. W. Wilson, 2011: Observations of elevated convection initiation leading to a surface-based squall line during 13 June IHOP_2002. *Mon. Wea. Rev.*, **139**, 247–271, doi:10.1175/2010MWR3422.1.

McPherson, R. A., and Coauthors, 2007: Statewide monitoring of the mesoscale environment: A technical update on the Oklahoma Mesonet. *J. Atmos. Oceanic Technol.*, **24**, 301–321, doi:10.1175/JTECH1976.1.

Moore, J. T., F. H. Glass, C. E. Graves, S. M. Rochette, and M. J. Singer, 2003: The environment of warm-season elevated thunderstorms associated with heavy rainfall over the central United States. *Wea. Forecasting*, **18**, 861–878, doi:10.1175/1520-0434(2003)018<0861:TEOWET>2.0.CO;2.

Pu, B., and R. E. Dickinson, 2014: Diurnal spatial variability of Great Plains summer precipitation related to the dynamics of the low-level jet. *J. Atmos. Sci.*, **71**, 1807–1817, doi:10.1175/JAS-D-13-0243.1.

Riley, G. T., M. G. Landin, and L. F. Bosart, 1987: The diurnal variability of precipitation across the central Rockies and adjacent Great Plains. *Mon. Wea. Rev.*, **115**, 1161–1172, doi:10.1175/1520-0493(1987)115<1161:TDVOPA>2.0.CO;2.

Rochette, S. M., and J. T. Moore, 1996: Initiation of an elevated mesoscale convective system associated with heavy rainfall. *Wea. Forecasting*, **11**, 443–457, doi:10.1175/1520-0434(1996)011<0443:IOAEMC>2.0.CO;2.

Schumacher, R. S., and R. H. Johnson, 2005: Organization and environmental properties of extreme-rain-producing mesoscale convective systems. *Mon. Wea. Rev.*, **133**, 961–976, doi:10.1175/MWR2899.1.

Shapiro, A., E. Fedorovich, and S. Rahimi, 2016: A unified theory for the Great Plains nocturnal low-level jet. *J. Atmos. Sci.*, **73**, 3037–3057, doi:10.1175/JAS-D-15-0307.1.

Sun, J., and F. Zhang, 2012: Impacts of mountain-plains solenoid on diurnal variations of rainfalls along the mei-yu front over the East China Plains. *Mon. Wea. Rev.*, **140**, 379–397, doi:10.1175/MWR-D-11-00041.1.

Surcel, M., M. Berenguer, and I. Zawadzki, 2010: The diurnal cycle of precipitation from continental radar mosaics and numerical weather prediction models. Part I: Methodology and seasonal comparison. *Mon. Wea. Rev.*, **138**, 3084–3106, doi:10.1175/2010MWR3125.1.

Trier, S. B., and D. B. Parsons, 1993: Evolution of environmental conditions preceding the development of a nocturnal mesoscale convective complex. *Mon. Wea. Rev.*, **121**, 1078–1098, doi:10.1175/1520-0493(1993)121<1078:EOECPT>2.0.CO;2.

——, C. A. Davis, D. A. Ahijevych, M. L. Wiseman, and G. H. Bryan, 2006: Mechanisms supporting lone-lived episodes of propagating nocturnal convection within a 7-day WRF model simulation. *J. Atmos. Sci.*, **63**, 2437–2461, doi:10.1175/JAS3768.1.

——, ——, ——, and K. W. Manning, 2014: Use of the parcel buoyancy minimum to diagnose simulated thermodynamic destabilization. Part I: Methodology and case studies of MCS initiation environments. *Mon. Wea. Rev.*, **142**, 945–966, doi:10.1175/MWR-D-13-00272.1.

Tripoli, G. J., and W. R. Cotton, 1989: Numerical study of an observed orogenic mesoscale convective system. Part I: Simulated genesis and comparison with observations. *Mon. Wea. Rev.*, **117**, 273–304, doi:10.1175/1520-0493(1989)117<0273:NSOAOO>2.0.CO;2.

Tuttle, J. D., and C. A. Davis, 2006: Corridors of warm season precipitation in the central United States. *Mon. Wea. Rev.*, **134**, 2297–2317, doi:10.1175/MWR3188.1.

Wallace, J. M., 1975: Diurnal variations in precipitation and thunderstorm frequency over the conterminous United States. *Mon. Wea. Rev.*, **103**, 406–419, doi:10.1175/1520-0493(1975)103<0406:DVIPAT>2.0.CO;2.

Weckwerth, W. M., D. B. Parsons, S. E. Koch, B. B. Demoz, C. Flamant, B. Geerts, J. Wang, and W. F. Feltz, 2004: An overview of the international H_2O project (IHOP_2002) and some preliminary highlights. *Bull. Amer. Meteor. Soc.*, **85**, 253–277, doi:10.1175/BAMS-85-2-253.

Wexler, H., 1961: A boundary layer interpretation of the low-level jet. *Tellus*, **13**, 368–378, doi:10.3402/tellusa.v13i3.9513.

Wilson, J. W., and R. D. Roberts, 2006: Summary of convective storm initiation and evolution during IHOP: Observational and modeling perspective. *Mon. Wea. Rev.*, **134**, 23–47, doi:10.1175/MWR3069.1.

Wolyn, P. G., and T. B. McKee, 1994: The mountain–plains circulation east of a 2-km high north–south barrier. *Mon. Wea. Rev.*, **122**, 1490–1508, doi:10.1175/1520-0493(1994)122<1490:TMPCEO>2.0.CO;2.